Heliyon 10 (2024) e27119

Contents lists available at ScienceDirect

Heliyon

journal homepage: www.cell.com/heliyon

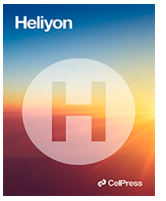

Review article

Review on the modifications of natural and industrial waste CaO based sorbent of calcium looping with enhanced CO_2 capture capacity

Nurfanizan Afandi [a,b,*], M. Satgunam [c], Savisha Mahalingam [a], Abreeza Manap [a,b], Farrukh Nagi [d], Wen Liu [e], Rafie Bin Johan [f], Ahmet Turan [g], Adrian Wei-Yee Tan [h], Salmi Yunus [i]

[a] *Institute of Sustainable Energy, Universiti Tenaga Nasional, Jalan IKRAM-UNITEN, 43000, Kajang, Selangor, Malaysia*
[b] *Department of Mechanical Engineering, College of Engineering, Universiti Tenaga Nasional, Jalan IKRAM-UNITEN, 43000, Kajang, Selangor, Malaysia*
[c] *Institute of Power Engineering (IPE), Universiti Tenaga Nasional, Jalan IKRAM-UNITEN, 43000 Kajang, Selangor, Malaysia*
[d] *UNITEN R&D Sdn Bhd, Universiti Tenaga Nasional, Jalan IKRAM-UNITEN, 43000, Kajang, Selangor, Malaysia*
[e] *School of Chemistry, Chemical Engineering and Biotechnology, Nanyang Technological University, 62 Nanyang Drive, Singapore, 637459, Singapore*
[f] *Nanotechnology and Catalysis Research Center (NANOCAT), University of Malaya, Kuala Lumpur, 50603, Malaysia*
[g] *Materials Science and Nanotechnology Engineering Department, Faculty of Engineering, Yeditepe University, 34755, Atasehir, Istanbul, Turkey*
[h] *Smart Manufacturing and Systems Research Group (SMSRG), University of Southampton Malaysia, Iskandar Puteri, 79100, Malaysia*
[i] *Materials Engineering and Testing Group, TNB Research Sdn Bhd, Kawasan Institusi Penyelidikan, No. 1 Lorong Ayer Itam, Kajang, 43000, Selangor, Malaysia*

A R T I C L E I N F O

Keywords:
Energy
Calcium looping cycle (CaL)
Natural sorbent
Industrial waste sorbent
High CO_2 capture capacity
High stability
Low cost

A B S T R A C T

The calcium looping cycle (CaL) possesses outstanding CO_2 capture capacity for future carbon-capturing technologies that utilise CaO sorbents to capture the CO_2 in a looping cycle. However, sorbent degradation and the presence of inert materials stabilise the sorbent, thereby reducing the CO_2 capture capacity. Consequently, the CaO sorbent that has degraded must be replenished, increasing the operational cost for industrial use. CaO sorbents have been modified to enhance their CO_2 capture capacity and stability. However, various CaO sorbents, including limestone, dolomite, biogenesis calcium waste and industrial waste, exhibit distinct behaviour in response to these modifications. Thus, this work comprehensively reviews the CO_2 capture capacity of sorbent improvement based on various CaO sorbents. Furthermore, this study provides an understanding of the effects of CO_2 capture capacity based on the properties of the CaO sorbent. The properties of various CaO sorbents, such as surface area, pore volume, particle size and morphology, are influential in exhibiting high CO_2 capture capacity. This review provides insights into the future development of CaL technology, particularly for carbon-capturing technologies that focus on the modifications of CaO sorbents and the properties that affect the CO_2 capture capacity.

* Corresponding author. Institute of Sustainable Energy, Universiti Tenaga Nasional, Jalan IKRAM-UNITEN, 43000, Kajang, Selangor, Malaysia.
E-mail address: Nurfanizan@uniten.edu.my (N. Afandi).

https://doi.org/10.1016/j.heliyon.2024.e27119
Received 23 September 2023; Received in revised form 6 February 2024; Accepted 23 February 2024
Available online 24 February 2024

1. Introduction

In 2022, global energy-related CO_2 emissions had grown by 0.9% compared with 2021, reaching a new high of more than 36.8 giga tonnes of CO_2 emissions due to high energy demand, mainly produced from fossil fuels [1]. To comply with the Paris Agreement [2], which aims to keep the rise in mean global temperature below 2 °C, countries such as Malaysia intend to reduce carbon emissions by 45% by 2030 [2]. Globally, many methods, such as introducing carbon taxation/trading schemes [3,4], renewable energy [5–7], improving efficiency [8] and carbon-capturing technology [9–11], have been introduced to reduce CO_2 emissions. However, fossil fuel usage is inevitable for the industry, especially in Malaysia, due to high energy generation that leads to high amounts of electricity generated at once [12]. Thus, carbon-capturing technology is foreseen to benefit industries, and the release of CO_2 is unavoidable during combustion.

Carbon capture technology consists of three leading technologies such as post combustion [13], pre combustion [14], and oxyfuel combustion [15]. Post combustion CO_2 technology, such as amine scrubbing, is the most mature in the industry because it generates less energy penalty and can easily retrofit into the existing power plant system [16]. However, cost becomes a major concern for amine scrubbing and limits the prospects of scaling up this technology for huge power plants. Therefore, calcium looping technology (CaL) has gained the interest of many researchers for low-cost post combustion CO_2 technologies.

The conceptual study of CaL technology was first introduced by Shimizu et al., in 1999 [17] for CO_2 removal from the combustion process. Over the years, the development of CaL from microscale studies in thermal gravimetric analysers to the modelling, simulation and economic feasibility, as well as bench-scale setups, had been explored for the development of CaL systems [14–17]. CaL pilot scales revealed that CaL benefits the industry in many aspects, mainly in cost and versatility.

The versatility of CaL is its ability to integrate into systems, such as power plants and cement power plants, for CO_2 emissions reduction and thermochemical energy storage [18–24]. In addition, CaL offers the following: (i) low-cost sorbents, such as limestone [25]; (ii) simultaneous partial desulphurisation from flue gases [26]; (iii) spent sorbents holding the potential to be used elsewhere or regenerated [27]; (iv) low energy penalty (approximately 6–8% [28]) than amine scrubbing technology (8.4%) [29]; (v) CO_2 transformation into a valuable gas with a CO_2 conversion exceeding 75% to achieve carbon neutrality, a vital goal for sustainable future development [30]; and (vi) high theoretical CO_2 capture capacity of pure CaO: 0.786 kg CO_2/kg sorbent. Although CaL can demonstrate high theoretical CO_2 capture capacity, the 0.786 kg CO_2/kg sorbent is based on pure CaO sorbent, where most sorbents contain inert materials that contribute to low CO_2 capture capacity. Therefore, achieving the highest CO_2 capture capacity theoretically is the main challenge due to the sorbent degradation and the presence of inert materials to maintain the stability of sorbents over the carbonation/calcination cycles.

Consequently, researchers exerted great effort to overcome this degradation and reported their studies in articles and journals since 1999 because sorbent degradation causes high operating costs, low CO_2 capture capacity, and low stability of the CaO sorbent, thus increasing the replenishment of sorbents. The most recent improvement involves binary reinforcement where two inert materials were combined together with CaO sorbent [31], nano CaO [32], and biomass and cement doped with calcium-based sorbents [33].

In this regard, the development of the CaO sorbent has been reviewed consistently during the previous decade, as summarised in Table 1 (obtained from the Web of Science since 2010). As shown in Table 1, state-of-art methods in improving the degradation have been reported since 2010 until the current year; these methods include acid modification, doping, treatment, use of synthetic sorbents

Table 1
Summary of the review paper related to development/improvement of CaO based sorbents.

Source	Publication Year	Review scope	Ref
Blamey et al.	2010	Review on the reducing the sorbent deactivation by thermal pretreatment, chemical doping, synthetic, and natural sorbent	[35]
Liu et al.	2012	Summarizes the state-of-the art research in the literature aiming to identify potential solutions to the loss-in-capacity of CaO based problem	[36]
Valderve et al.	2013	Review on the novel Ca-based sorbents with improved thermal and mechanical stability.	[37]
Erans et al.	2016	Review on techniques to enhance natural sorbent performance, synthetic sorbent, reactivation, and re-use deactivated materials	[34]
Perejon et al.	2016	Summary on the effects of recarbonation and thermal/mechanical pretreatment for sorbent reactivation at CaL conditions, and on the demonstration of the technology in pilot-plants	[38]
Sun et al.	2018	Review on improvement of CaO-based adsorbents for CO_2 capture (e.g. surface modification and dispersing on inert supports) Review on the effects of operation conditions (e.g. CO_2 partial pressure, carbonation temperature, carbonation time, and contaminants) on the cyclic performance of carbonation and calcination. Review the attrition in real applications	[39]
Hu et al.	2020	Review on the recent advances in the developments of inert support incorporated CaO sorbents for high temperature CO_2 capture	[40]
Chen et al.	2020	Review on recent development of advancement in the design and reinforcement of CaO based sorbent with an emphasis on its development in China	[28]
Dunstan et al.	2021	Review on the fundamental aspects underpinning solid CO_2 sorbent based on alkali and alkaline earth metal oxides. Review on the influence of material structure, ionic conduction, and particle morphology, on CO_2 absorption of a Ca-based, Mg-based, and Li-based.	[41]

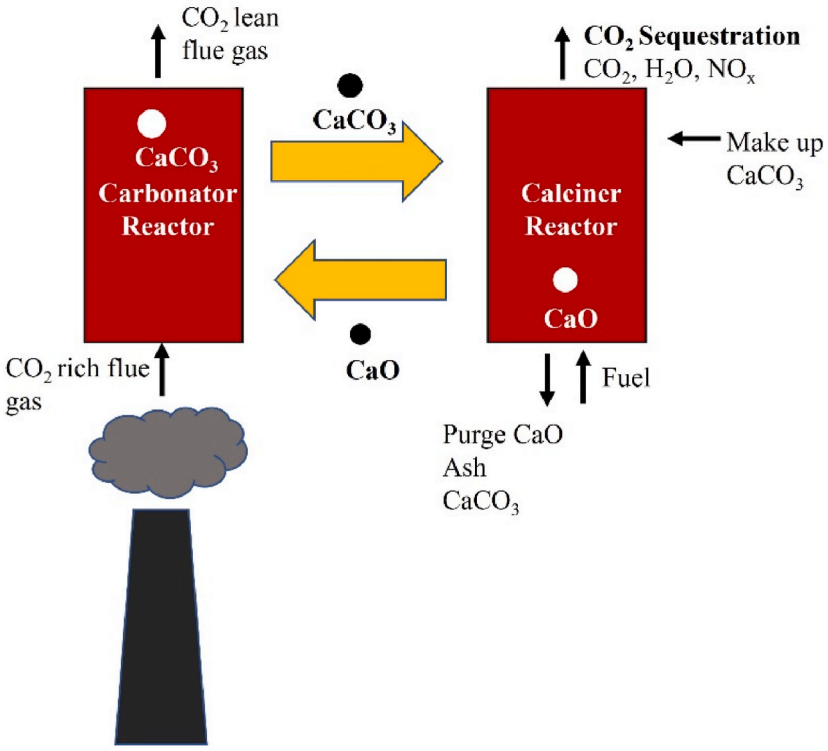

Fig. 1. Schematic diagram of Calcium Looping Cycle (CaL).

and, alteration of the operating conditions on the cyclic performance of carbonation and calcination and the influence of material structure based on the type of sorbent [28,34–41]. However, these review papers mainly cover the modification by generalising the type of CaO sorbents.

Various CaO sorbents demonstrate different CO_2 capture capacities due to distinct parameters, such as pore structure generated from releasing gases such as CO_2 during calcination [42]. Using calcium gluconate as CaO sorbent exhibits higher specific surface area, 16.4 m^2/g than calcium acetate which yields a high CO_2 capture capacity, 0.75 g CO_2/g sorbent, nearly the theoretical CO_2 capture capacity of pure CaO. Meanwhile, acid modifications improve the porosity of the CaO sorbent and enhance the cyclic CO_2 capture capacities [43]. Acid modifications using various acids demonstrate different CO_2 capture capacities due to diverse surface areas [44]. Moreover, doping enhances structural stability by increasing the adsorption energy of CaO surfaces. Zhao et al. (2024) [45] found that the adsorption energy of CaO clusters on $Ca_3Al_2O_6$ is −5.66 eV, which is 2.4 times higher than that on the CaO surface and causes only a slight drop in CO_2 capture capacity at 30 cycles.

Moreover, limestone with 40% of Bayer aluminium hydroxide (BAh) demonstrates higher surface area and pore volume (i.e. 36.0 m^2/g and 0.141 cm^3/g, respectively) than other BAh compositions [46]. Unfortunately, the CO_2 capture capacity of 40% of Bah exhibits the lowest CO_2 capture capacity than other BAh compositions which contradicts previous studies. Thus, further clarifications and investigation must be made on the properties that can affect CO_2 capture capacity.

Therefore, this study comprehensively reviews the effect of CO_2 capture capacity of sorbent modifications based on the sorbent type. Moreover, to the author's best knowledge, no review has been conducted on the effect of CO_2 capture capacity based on the properties of CaO sorbents. Previous studies generalised the properties based on a general statement, such as high surface area and pore volume exhibiting high CO_2 capture capacity. By contrast, this review provides insight into the future development of CaL technology, particularly for carbon-capturing technology that mainly focuses on modifying CaO sorbents and the properties that affect the CO_2 capture capacity.

2. Calcium looping

The CaL cycle consists of two interconnected circulating reactors: carbonator and calciner, as shown in Fig. 1. In the carbonator, the CO_2 from flue gases reacts with the calcium oxide (CaO) sorbent to form calcium carbonate ($CaCO_3$) between 600 °C and 700 °C (Equation (1)). Then, the CO_2 lean flue gas is directed to the outlet. The formed $CaCO_3$ flows to the calciner reactor and is calcined to break the bond of $CaCO_3$ to become CaO and CO_2 (Equation (2)). The CaO is circulated back to the carbonator for the next cycle, and the obtained pure CO_2 is ready for final purification, compression, and storage. CaL is a reversible reaction of CaO sorbent involving high-reaction enthalpy, where $\Delta H^{\circ}_{298K} = -178$ kJ/mol at 298 K as shown in Equations (1) and (2).

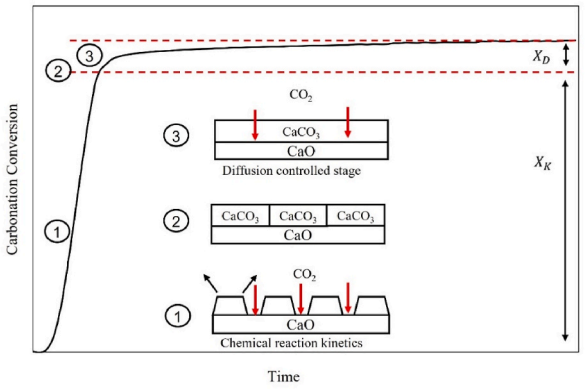

Fig. 2. Schematic diagram of carbonation conversion during carbonation reaction. Reproduced from Ref. [34].

$$CaO + CO_2 \rightarrow CaCO_3 \quad \Delta H^{\circ}_{298K} = -178 \text{ kJ} / \text{mol} \tag{1}$$

$$CaCO_3 \rightarrow CaO + CO_2 \quad \Delta H^{\circ}_{298K} = +178 \text{ kJ} / \text{mol} \tag{2}$$

The types of CaO sorbents used in CaL are (i) natural, (ii) industrial waste, and (iii) synthetic. Natural sorbents include limestone, dolomite, biogenesis calcium waste, and mangano calcite. Meanwhile, industrial waste consists of lime mud (LM), carbide slag (CS), blast furnace slag (BFS), and waste marble powder (WMP). Synthetic sorbents are produced using synthetic methods such as sol-gel [47], co-precipitation [48], wet mixing [49], granulation [50], template [51], impregnation [52] and flame spray pyrolysis [53] from various CaO precursors such as calcium nitrate ($Ca(NO_3)_2$), calcium gluconate ($C_{12}H_{22}CaO_{14}$), calcium acetate ($Ca(C_2H_3O_2)_2$), and calcium carbonate ($CaCO_3$).

However, the CO_2 capture capacity of CaO sorbents degrades rapidly after several cycles in CaL. Sorbent degradation means the sorbent could not maintain its carbonation conversion or CO_2 capture capacity over the carbonation/calcination cycles, which affect the sorbent stability. The leading causes of this degradation include the attrition and sintering effect of CaO sorbents [34]. Attrition occurs because of the mechanical motion and the temperature or the pressure gradient inside the particles that are subjected to the fast environment changes that are developed during calcination carbonation. This phenomenon is influenced by the design of the system, such as reactor configurations, properties of the solid, and reacting environment [54]. Meanwhile, the sintering effect is a change in pore shape, pore shrinkage, and grain growth, mainly occurring during calcination due to the presence of heat [34,55,56]. The sintering effect occurs at high calcination temperatures, reducing the carbonation conversion of sorbent inside the carbonator reactor and leading to a high degradation rate. In addition to attrition and the sintering effect, some of the degradations can be related to the closure of pores smaller than 300 nm [57] during carbonation that does not reopen during the subsequent cycles [34]. This degradation makes the sorbent unable to maintain the stability of the sorption performance after many cycles. This inability leads to sorbent replacement which is undesired due to additional operating costs [58]. Thus, the carbonation and calcination reactions are explained in the next session to understand the degradation behaviour.

2.1. Carbonation reaction

Referring to Equation (1), the carbonation reaction happens when the CaO reacts with CO_2 to form $CaCO_3$. The carbonation reaction consists of two stages: chemical reaction kinetics that control the initial and fast stage, followed by the solid diffusion-controlled stage to form the $CaCO_3$ at the slow stage as shown in Fig. 2. X_K is the molar conversion under the fast reaction regime and X_D is the molar conversion under the diffusion-controlled stage. The carbonation reactions start with the CO_2 reacting on the CaO-free surface to become the $CaCO_3$ at a fast carbonation rate due to numerous CaO-free surfaces. Then, the reaction reaches the limits when there is no CaO-free surface for CO_2 to react with. Finally, the $CaCO_3$ starts forming a layer, and the diffusion stages slow down at a certain thickness of $CaCO_3$ layer due to the lack of active CaO to react with CO_2 to become $CaCO_3$. The thickness of the product layer varies between 22 and 90 nm based on the properties of sorbent and operating conditions [59,60].

The sorption performance can be analysed in terms of carbonation conversion or CO_2 capture capacity. The equations for carbonation conversion and CO_2 capture capacity as shown in Equations (3) and (4), respectively.

$$CO_2 \text{ capture capacity} = \frac{\text{weight of captured } CO_2}{\text{weight of sorbent}} = \frac{m_f - m_0}{m_0} \tag{3}$$

$$\text{Carbonation conversion} = \frac{\text{mol of reacted CaO}}{\text{mol of sorbent}} = \frac{(m_f - m_0)/44}{m_0/56 \times x} \tag{4}$$

where m_f is the mass of the sorbent at the end of carbonation at each cycle, m_0 is the initial mass at each cycle, and x is the mass fraction

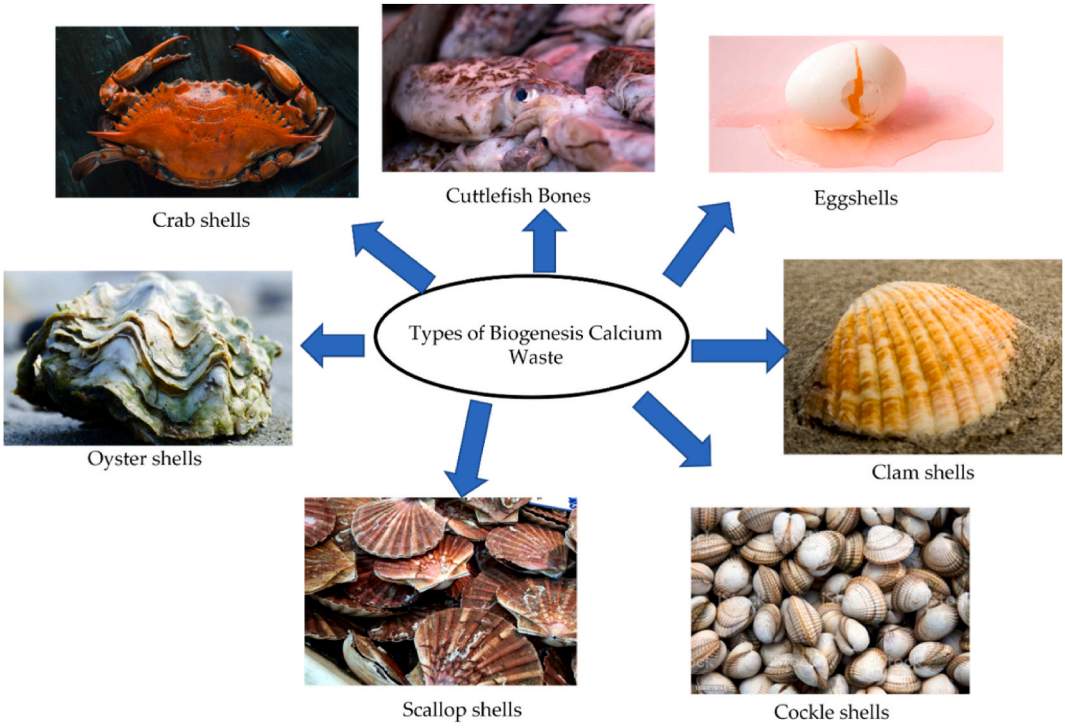

Fig. 3. Type of biogenesis calcium waste.

of the active CaO in the cycle.

2.2. Calcination reaction

Calcination reaction is an endothermic process where additional fuel is necessary to achieve a rapid reaction at 850 °C–950 °C without excessive sintering. Equation (2) shows the calcination reaction where the $CaCO_3$ must be heated to break into CaO and CO_2. Theoretically, pure CO_2 stream outlet production is at 900 °C under atmospheric conditions. Even though the high calcination temperature (900 °C) is favourable in reaction kinetics, it can lead to the sintering effect where the pore shape of $CaCO_3$ is affected, leading to the grain growth of $CaCO_3$. The sintering effect occurs when the sintering temperature exceeds the Tammann temperature of the sorbent, which is generally 50%–75% of the melting point temperature of the sorbent [61]. At this stage, the grain boundary integrates and causes agglomeration due to the activation of the diffusion of ions and cavities that leads to a reduction in surface area and reduction in CO_2 capture capacity. The Tammann temperature of $CaCO_3$ is 533 °C [62] and exceeding this temperature causes the sintering effect and degrades the sorbent performance in CaL.

3. Classification of CaO-based sorbents

Based on previous literature review, the different types of CaO sorbent precursors exhibits various carbonation conversion or CO_2 capture capacity. In this review, the approach suggested by Chen et al. (2020) [28], and Erans et al. (2016) [34] is used to classify the resources of CaO sorbent precursors based on the originality of resources. The type of resources is classified into two categories, i.e. natural, and industrial waste. Thus, this part focuses on the general introduction and the drawbacks of the various type of CaO sorbents.

3.1. Natural CaO sorbent

Natural CaO sorbents include limestone, dolomite and other natural materials, such as biogenesis calcium waste and mangano calcite material.

Limestone is widely used as a CaO sorbent in the CaL cycle due to its non-toxic properties, availability and low cost [63]. The cost of limestone is reported to be approximately $110/tonnes [64]. Limestone is a sedimentary rock that consists of more than 95% calcium carbonate, $CaCO_3$, which has a typical carbonation conversion of 80% on the first cycle but drops at approximately 15%–20% after the subsequent cycle [35]. The low stability especially after 20 cycles is mainly attributed to the sorbent sintering and pore blocking under mild calcination temperature, i.e. in between 750 °C and 900 °C [65]. The sintering effect is attributed to the loss of micropores and mesopores, which then causes the reduction in surface area and total pore volume. The carbonation conversion of limestone decreases

Table 2
CO_2 capture capacity for different types of natural CaO precursors.

Natural CaO sorbent	Powder size	Process condition		Cycles	Surface area (m^2/g)		Pore volume (cm^3/g)		Sorption Performance (g CO_2/g sorbent)		Deactivation (%)	Ref
		Carbonation	Calcination		Initial	Final	Initial	Final	Initial	Final		
Limestone	125–250 μm	At 700 °C, for 20 min, under 15 vol% CO_2	At 900 °C, for 20min, under 80 vol% CO_2	20	10.0	3.4	0.040	0.0004	0.45	0.10	78.0	[65]
Mangano calcite	–	At 650 °C, for 20 min, under 15 vol% CO_2/85 vol % N_2	At 900 °C, for 10min, under 100 vol% N_2	20	8.9	5.2	–	–	0.38	0.23	40.0	[77]
Limestone	150–180 μm	At 850 °C, for 20 min, under 100 vol% CO_2	At 725 °C, for 5min, under 100 vol% N_2	20	11.4	–	0.066	–	0.61	0.33	45.9	[79]
Dolomite	150–180 μm	At 850 °C, for 20 min, under 100 vol% CO_2	At 725 °C, for 5min, under 100 vol% N_2	20	29.5	–	0.195	–	0.45	0.40	11.1	[79]
Biogenesis calcium waste – Eggshells	–	At 700 °C, for 10 min, under CO_2	At 900 °C, for 5min	10	–	–	–	–	0.23	0.10	56.5	[80]
Biogenesis calcium waste –Chicken Eggshells	–	At 700 °C, for 20 min, under 15 vol% CO_2/85 vol % N_2	At 850 °C, for 10min, under 100 vol% N_2	20	15.2	–	0.08	–	0.47	0.15	66.7	[81]
Biogenesis calcium waste –Cockle shells	–	At 800 °C, under 100 vol% CO_2	At 850 °C, for 20min, under 100 vol% N_2	9	–	–	–	–	0.51	0.20	61.5	[82]

Table 3
Analysis of sorbent composition.

CaO sorbent	Composition (wt%)						Ref
	CaO	MgO	SiO_2	CO_2[b]	Loss on Ignition (LOI)[a]	Others	
Limestone	55.92	0.37	0.18	–	43.46	0.07	[54]
Purbeck limestone	53.49	0.50	1.30	41.97	–	2.74	[83]
Limestone	55.27	0	0.58	–	43.92	0.23	[46]
Dolomite	36.02	12.47	1.13	–	43.04	7.34	[84]
Dolomite	32.20	10.90	24.10	–	22.0	10.80	[85]
[c]Calcined eggshells	97.08	0.54	1.27	–	–	1.07	[86]
[c]Calcined duck eggshells	97.81	0.66	0.26	–	–	1.27	[87]
Waste Marble Powder	54.50	0.90	0.80	–	42.85	0.95	[88]
[d]Blast Furnace Slag	36.84	10.14	34.27	–	–	18.75	[89]

[a] LOI = Loss on ignition from XRF analysis due to the presence of volatile components.
[b] CO_2 = One of the volatile components that contribute to the LOI.
[c] Low LOI is detected on the calcined samples due to the exposure to high temperatures causing the expulsion of volatile components.
[d] Low LOI is detected leading to minimal mass loss during ignition where no volatile components are present.

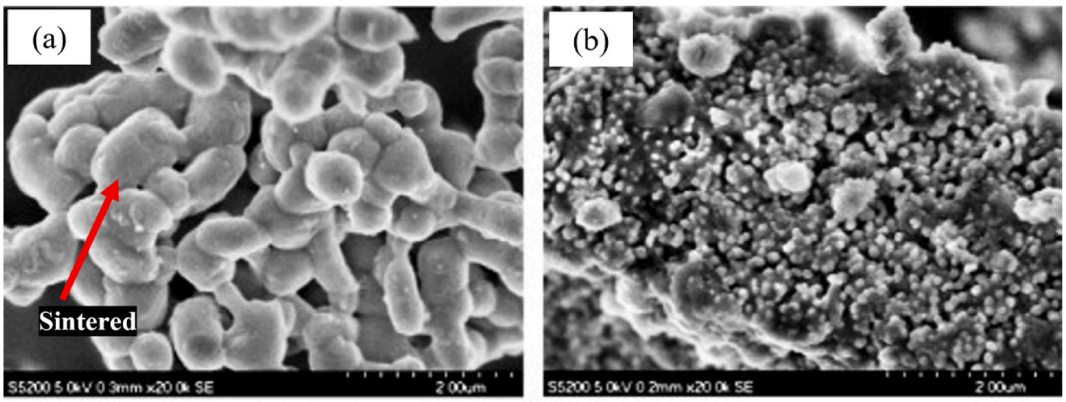

Fig. 4. SEM pictures of (a) limestone and (b) dolomite samples after being subjected to carbonation/recarbonation/calcination cycles (precalcined, air 850 °C and regenerated by calcination under 70% CO_2 at 950 °C). Reproduced from Ref. [78].

more rapidly at high calcination temperatures (above 900 °C) due to the sintering effect [66].

Meanwhile, dolomite is abundant on Earth. It is a carbonate material that is composed of calcium magnesite carbonate, and it is a good alternative for low-cost, calcium-based CaO sorbents. The cost of dolomite is estimated to be approximately $100/tonnes [64]. Thus, it is suitable to be used for large-scale production where the cost of the raw material is cheap, thus reducing the production cost. The CaO content in dolomite is approximately 37%, which is lesser than limestone [67]. This content contributes to a low initial CO_2 capture capacity, although dolomite has higher stability than limestone. The presence of magnesium oxide (MgO) in the CaO sorbent, which is inert and capable of producing a high skeleton structure of sorbents, increases the regenerability and stability of sorbents after several cycles under mild conditions [68,69]. This skeleton structure obstructs the aggregation or sintering of CaO during calcination [70]. In addition, MgO has a high Tammann temperature (1276 °C), which helps the sorbent suppress the sintering effect during calcination [71]. Moreover, Teixiera et al. (2021) [72] discovered that the deactivation of dolomite after 20 cycles of carbonation at 700 °C under mild calcination conditions was 34%, which is lesser than that of limestone. Nevertheless, the performance of the dolomite is affected by high calcination temperature because the MgO skeleton can no longer efficiently prevent crystal sintering. Thus, it reduces the surface area of the dolomite, decreasing the CO_2 capture capacity and carbonation conversion after several cycles.

In addition to limestone and dolomite, biogenesis calcium waste such as eggshell, shellfish, cuttlefish bones, clam shells, cockle shells, scallop shells, crab shells, and oyster shells has been proposed for the type of CaO sorbent in the CaL cycle [73]. Fig. 3 shows several examples of these biogenesis calcium wastes. This alternative was introduced because natural resources, such as limestone and dolomite, are non-renewable and energy-intensive to exploit; moreover, the mining process is harmful to the environment and landscape [74]. Eggshells demonstrate a high CO_2 capture capacity, and a conversion of 76.41% after the first cycle which is close to the theoretical CO_2 capture capacity of CaO, i.e. 78.5% under mild conditions, which the calcination temperature at 825 °C. However it diminishes in subsequent cycles (conversion of 43.98%) due to sintering and attrition/fragmentation [75,76].

In addition, using mangano calcite as sorbent exhibits better cyclic performance for CO_2 capture capacity and carbonation conversion than limestone, even under various calcination conditions [77]. The mangano calcite is composed of CaO and calcium manganese oxide (Ca_2MnO_4), where Ca_2MnO_4 in calcined mangano calcite promotes the sorbent's excellent anti-sintering properties. However, resources for mining mangano calcite are limited.

Table 4
Comparison between industrial waste.

CaO sorbent	CaO content (%)	Powder size	Process condition		Cycles	Surface area (m^2/g)		Pore volume (cm^3/g)		Sorption Performance (g CO_2/g sorbent)		Deactivation (%)	Ref
			Carbonation	Calcination		Initial	Final	Initial	Final	Initial	Final		
Carbide Slag	73.88	105 μm	At 750 °C, under 30 vol% CO_2/ 70 vol % N_2	At 900 °C, under 100 vol % N_2	20	18.4	–	0.133	–	0.41	0.32	21.95	[81]
Lime Mud	52.54	0.125 mm	At 700 °C, for 30 min, under 15 vol% CO_2/85 vol % N_2	At 850 °C, for 10min, under 100 vol% N_2	30	6.2	–	0.016	–	0.33	0.07	77.5	[93]
Blast Furnace Slag – leached with nitric acid	40.94	0.05–0.1 mm	At 650 °C, for 10 min, under 20 vol% CO_2/80 vol % N_2	At 900 °C, for 5min, under 100 vol% N_2	20	–	–	–	–	0.37	0.23	37.83	[100]
Waste Marble Powder	28.27	<170 μm	At 650 °C, for 30 min, under 15 vol% CO_2/85 vol % N_2	At 850 °C, for 5min, under 100 vol% N_2	20	6.0	–	–	–	0.63	0.25	60.3	[105]

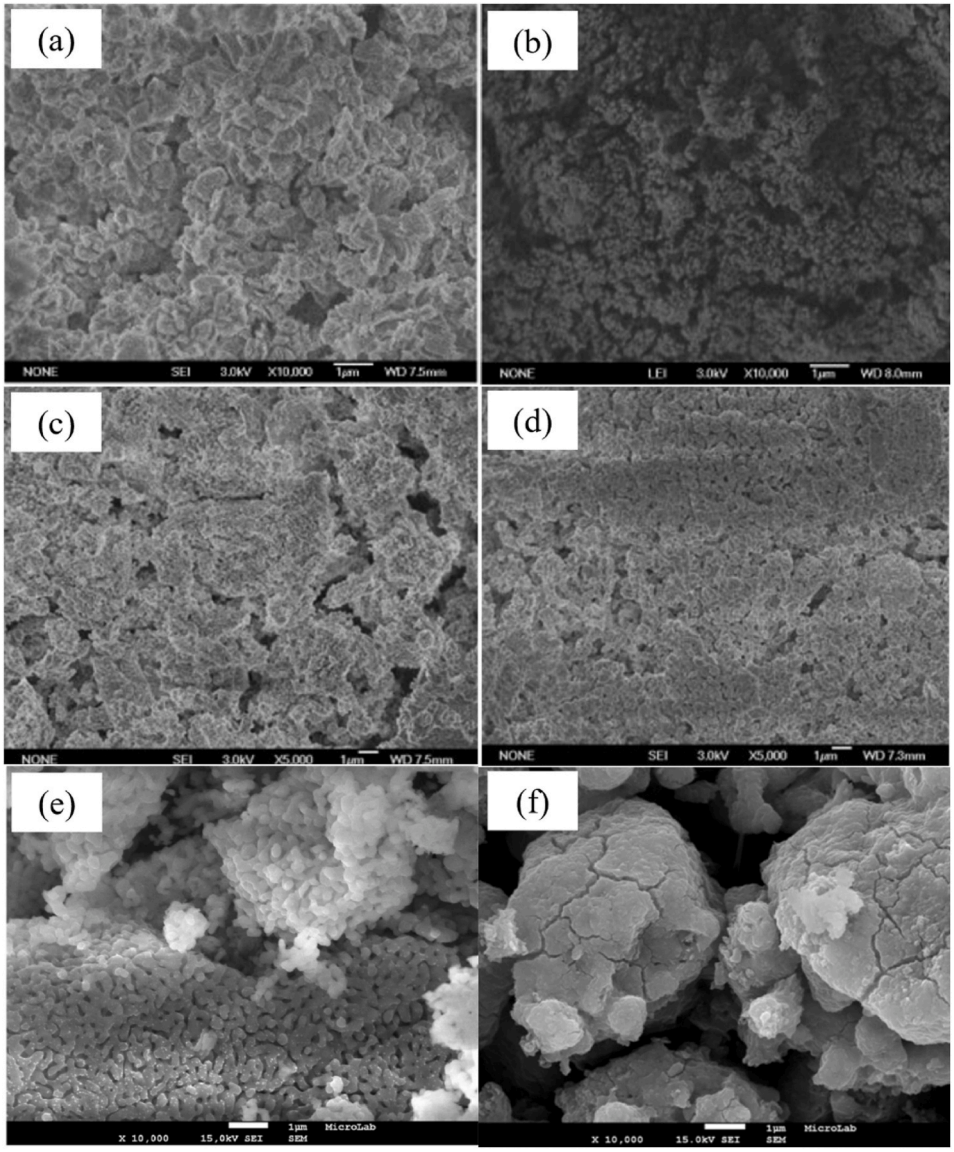

Fig. 5. SEM pictures of (a) LM, 1st cycles, (b) LM after 100 cycles (c) CS after 1 cycle (d) CS after 10 cycle (e) fresh WMP (f) WMP after 20 cycles. Reproduced from Ref (a),(b) [92], (c),(d) [104], (e),(F) [102].

Table 2 shows that limestone has the highest initial CO_2 capture capacity amongst natural sorbents due to its more active and higher CaO content presence compared with other sorbents, as shown in Table 3. However, limestone degrades rapidly after 20 cycles. Meanwhile, dolomite exhibits high stability amongst these sorbents due to presence of MgO but with low initial CO_2 capture capacity due to the low percentages of CaO. The presence of MgO skeleton improves the stability of dolomite. Fig. 4(a) and (b) shows the morphology of limestone and dolomite, respectively when subjected to carbonation/calcination cycles using scanning electron microscopy (SEM). The morphology of limestone is markedly sintered, resulting in the reduction in the reactive surface area, which causes low stability after several cycles. Meanwhile, the cycled dolomite exhibits higher porosity and the MgO grains are segregated from sintered CaO and appear to be resistant to sintering [78]. Even though eggshells have the highest CaO content amongst other sorbents, they exhibit lower initial CO_2 capture performance than limestone, probably due to less active CaO presence in an eggshell. The improvement of these natural sorbents is discussed in Section 4.0.

3.2. *Industrial waste CaO sorbent*

Industrial waste CaO sorbents, such as LM, CS, BFS and WMP, are widely used in CaL.

LM is a solid waste from the paper mill industry that is useful in CaL because the main component is $CaCO_3$ [90,91]. LM can achieve

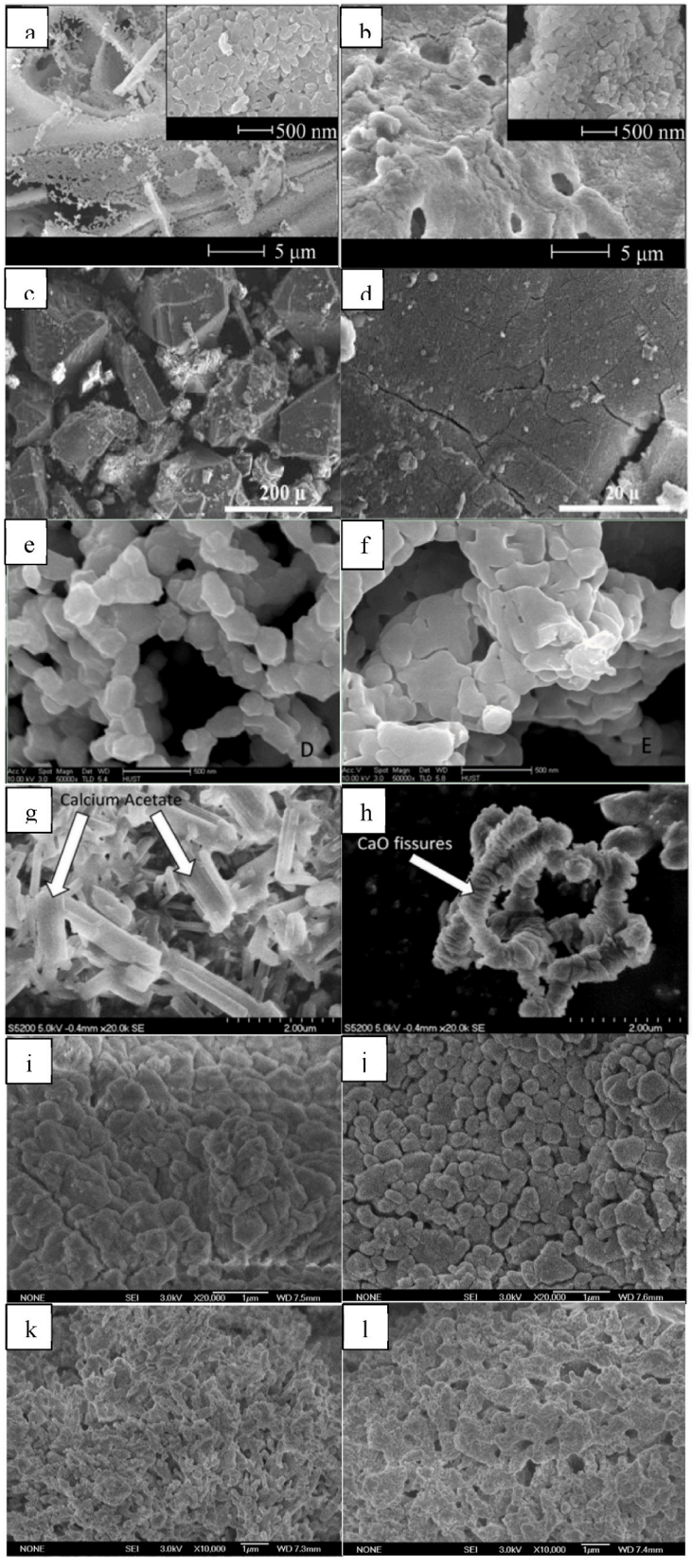

(caption on next page)

Fig. 6. SEM images of the acid-modified limestone (a) Fresh GA (GA) (b) GA 10 cycles (c) Fresh FA (d) calcined FA (e) Fresh TA (f) TA 26 cycles (g) Fresh AA (h) AA 20 cycles (i) Fresh PA (j) PA 100 cycles (k) PrA 1 cycle (l) PrA 26 cycles. Reproduced from (a),(b) from Ref. [113], (c), (d) from Ref. [106], (e),(f) from Ref. [109], (g),(h) from Ref. [110], (i),(j) from Ref. [112], (k)(l) from Ref. [111]).

the highest carbonation conversion when carbonated at 700 °C, but the carbonation conversions decrease with the increase in calcination temperature from 850 °C to 1000 °C [92]. Moreover, LM exhibits lower carbonation conversion than limestone due to the chlorine content in the lime mud [92,93]. The increase in chlorine content causes a decrease in pore volume and surface area by 71.3% and 44.5%, respectively, and limits the CO_2 diffusion and carbonation reaction during carbonation. Thus, the pre-washed process of LM can remove the chlorine during the preparation of sorbent and enhance the CO_2 capture capacity [93]. However, LM still demonstrates slow carbonation rate during chemical reaction stages and high carbonation rate during solid diffusion-controlled stages. This prolonged carbonation duration is not favourable in actual condition of CaL.

The CS is one of the industrial wastes generated by the production of acetylene gas (C_2H_2) and contains $Ca(OH)_2$ as the primary material. Approximately 75 million tonnes of global PVC production was generated in 2021 [94,95]. It has caused severe environmental pollution and land waste because the carbide slag is disposed of at a landfill near a chlor alkali plant [96,97]. CS demonstrates a high stability of CO_2 capture capacity due to the calcium hydroxide ($Ca(OH)_2$) composition undergoing dehydration during the calcination process to form CaO [94]. However, the initial CO_2 capture capacity is 0.42 g CO_2/g sorbent, which is lower than that of limestone.

In addition, the BFS is introduced as a potential CaO sorbent. It is a non-biodegradable waste material from steel and iron production [98]. Approximately the production of BFS exceeds several dozen million tonnes (about 25 million) annually [99] and waste control of the BFS is crucial to reducing environmental pollution. The BFS is calcium, Ca– and silica, Si–rich and is contemplated to be used as CaO-based sorbent. However, acid is used to activate the BFS as CaO sorbent, called the leaching process. During this process, the concentration of nitric acid (NA) and duration of shaking must be at the optimum condition of 3 mol/L and 120 min, respectively [100]. Leaching is important because carbide furnace slag has a limited pore structure of BFS, which limits adsorption efficiency and thus restricts the CO_2 capture capacity [101]. However, leaching can contribute to additional costs due to acid usage, which is also not environmentally friendly. Furthermore, WMP is introduced as another CaO sorbent.

WMP is generated after the cutting and polishing procedures of the marble rock. An estimated 20% of the total marble handles is transformed into waste; a marble producer plant produces about 250–400 tonnes of WMP annually [102]. The disposable components of WMP becomes a huge concern because it is landfilled, leading to severe environmental pollution. Similarly, the usage of WMP as CaO sorbent in CaL results in high initial carbonation conversion. The reactivity of cyclic stability decreased from 68% (first cycle) to 53% (20 cycles) compared with calcite that was obtained from a company called Cimentos de Portugal, E.P. (CIMPOR) [103].

Industrial waste becomes an alternative type of CaO precursor in CaL. Using industrial waste in CaL can reduce landfills and the cost of CaO precursors. As shown in Table 4, the WMP exhibits a high CO_2 capture capacity of 0.63 g CO_2/g sorbent, but the degradation decreases considerably over the cycles, indicating low stability. Fig. 5(a) and (b) illustrate the morphology of LM after the first cycle, and it shows a compact structure, which indicates that the presence of chlorine aggravates its sintering during calcination. Meanwhile, the CS and BFS demonstrate high stability over the cycles and have low CO_2 capture capacity. However, LM produces large pores (>1000 nm) in the surface after 100 cycles, which is not beneficial to carbonation because the reduction in surface area causes less reaction to occur during carbonation [92]. Meanwhile, CS still appears compact and expensive after 10 cycles, which is beneficial for CO_2 diffusion as shown in Fig. 5(c) and (d) [104]. Fig. 5(e) and (f) show the dismantled aggregates of sintered particles with visible fissures and cracks after 20 cycles of WMP that is associated with the formation of mesopores which causes low stability [102]. Thus, improving these industrial wastes can improve the stability and CO_2 capture capacity of CaO sorbent.

4. Improvement of sorbent

Sorption performance has been substantially improved in terms of carbonation conversion and CO_2 capture capacity, and stability of the CaO sorbent. Hence, this part aims to provide details about the improvement for limestone, dolomite, biogenesis calcium waste and industrial waste.

4.1. Limestone

The degradation of limestone became noticeable over increasing numbers of carbonation/calcination cycles especially under high calcination temperature, i.e. more than 800 °C [66]. The sintering effect and closure of pores contributed to this degradation, thus reducing the CO_2 capture capacity and carbonation conversion. Several efforts had been made to improve this degradation, e.g. acid modifications, doping and various pre-treatment of sorbent.

4.1.1. Acid modifications of limestone

Different acids exhibit different sorption capacities in acid modifications, and the price of acid becomes a major concern. Therefore, organic acids were used in acid modifications.

4.1.1.1. Formic acid. Formic acid (FA) demonstrated a high CO_2 capture capacity, 0.6 g CO_2/g sorbent despite having low surface area and pore volume after acid treated as shown in Fig. 6(c) and demonstrate the outcome of compacted surface with few cracks after 20

Table 5
Limestone with acid modification.

Type of acids	Sorbent size	Process condition		Cycles	Surface area (m^2/g)		Pore volume (cm^3/g)		Sorption Performance (g CO_2/g sorbent)		Deactivation (%)	Ref
		Carbonation	Calcination		Initial	Final	Initial	Final	Initial	Final		
Formic acid	<53 μm	At 650 °C, for 20 min, under 15 vol% CO_2/ 85 vol% N_2	At 850 °C, for 5 min, under 100 vol% N_2	20	2.9	–	0.007	–	0.60 g CO_2/g sorbent	0.22 g CO_2/g sorbent	63.3	[106]
Various acid (Acetic acid, Formic acid, Vinegar, Oxalic acid)	<53 μm	At 650 °C, for 20 min, under 15 vol% CO_2/ 85 vol% N_2	At 850 °C, for 5 min, under 100 vol% N_2	20	2.7	–	0.009	–	0.54 g CO_2/g sorbent	0.23 g CO_2/g sorbent	57.4	[107]
Acetic acid	0.05–0.074 mm	At 700 °C, for 20 min, under 15 vol% CO_2/ 85 vol% N_2	At 850 °C, for 15 min, under 100 vol% N_2	10	17.5	11.0	0.210	0.145	94% Conversion	76% Conversion	19.1	[108]
Various organic acid (formic acid, acetic acid, propionic acid, citric acid, oxalic acid, lactic acid, malic acid, tartaric acid)	<150 μm	At 650 °C, for 30 min, under 15 vol% CO_2/ 85 vol% N_2	At 900 °C, for 10 min, under 100 vol% CO_2	26	13.2	–	–	–	82% Conversion	36% Conversion	56.1	[109]
Acetic acid	N/A	At 650 °C, for 30 min, under 15 vol% CO_2/ 85 vol% air	At 900 °C, for 5 min, under 70 vol% CO_2/ 30 vol% air	20	–	–	–	–	0.22 g CO_2/g sorbent	0.08 g CO_2/g sorbent	63.3	[110]
Propionic acid	<0.125 mm	At 700 °C, for 30 min, under 15 vol% CO_2/ 85 vol% N_2	At 850 °C, for 15 min, under 100 vol% N_2	10	11.3	5.2	0.064	0.022	98% Conversion	64% Conversion	34.5	[111]
Pyroligneous acid	<0.125 mm	At 700 °C, for 30 min, under 15 vol% CO_2/ 85 vol% N_2	At 850 °C, for 5 min, under 100 vol% N_2	20	13.8	5.0	0.117	0.090	75% Conversion	45% Conversion	40.0	[112]
Gluconic acid	N/A	At 700 °C, for 20 min, under 15 vol% CO_2/ 85 vol% N_2	At 950 °C, for 5 min, under 100 vol% CO_2	10	–	–		–	0.63 g CO_2/g sorbent	0.33 g CO_2/g sorbent	47.6	[113]
Acetic acid	N/A	At 650 °C, for 30 min, under 15 vol% CO_2/ 85 vol% N_2	At 850 °C, for 5 min, under 100 vol% N_2	20	–	–	–	–	80% Conversion	50% Conversion	37.5	[114]

cycles as shown in Fig. 6(d) [106]. However, the CO_2 capture capacity degrades rapidly after a few cycles similar to other acids due to the sintering effect [107]. Moreover, the concentrations of FA were found to have no remarkable effect due to the calcination of calcium formate. In addition, the mixtures of limestone with FA produce formaldehyde gas which is toxic and flammable and the usage of FA is not practical for safety purposes. Moreover, FA modification does not increase the surface area and pore volume, in contrast to other acid modifications.

4.1.1.2. Acetic acid. Acetic acid (AA) is commonly used as a modifier of limestone. The carbonation conversion of modified acetic acid is 2.33 higher than unmodified calcined limestone [108] and higher than other organic acids during the initial cycle [109]. This characteristic contributes to a high porous surface and small grain size due to the decomposition of calcium acetate into acetone, CO_2 and CaO [108]. Moreover, modified limestone with AA as sorbent can reduce the energy penalty when integrating with a power plant. However, these statements contradict when under realistic conditions (calcination at 900 °C to promote exothermic calcination reaction efficiently), where AA modification exhibits lower CO_2 capture capacity than natural limestone due to the sintering intersection from calcium acetate, as shown in Fig. 6(h) [110]. Essentially, the AA modification demonstrates grains with a rod-shape like, as shown in Fig. 6(g). Despite good performance when the calcination temperature is less than 900 °C, the high viscosity of AA still causes difficulties in transportation inside the reactor [111]. Moreover, the acetified sorbent enhances sulphation compared with non-acid-treated ones, such as pure limestone, and causes the irreversible formation of calcium sulfate ($CaSO_4$). Thus, AA treatment is not beneficial when sulphur dioxide (SO_2) is present in the flue gases [107].

4.1.1.3. Propionic acid. In addition to AA, propionic acid (PrA) modification enhances limestone's anti-sintering properties when calcined at 850 °C–950 °C [111]. The carbonation conversion of modified limestone with PrA is 3.9 times higher than unmodified limestone, even after 100 cycles. Fast carbonation rate and high conversions are exhibited with modified limestone due to a fluffier and porous structure than unmodified limestone, which promotes small diffusion resistance in the sorbent as shown in Fig. 6(k) and (l).

4.1.1.4. Pyroligneous acid. Pyroligneous acid (PA) can be an alternative to acetic acid. Modified PA demonstrated high carbonation conversion, which is four times higher than untreated limestone at a calcination temperature of 960 °C. The ratio of PA to limestone influences the CO_2 capture capacity where the optimal ratio is 20 mL/g. Treated sorbents exhibit better pore structure parameters, such as surface area, pore volume, and pore size distribution, than untreated limestone. However, it contains many impurities due to the sources of acid from acid waste and needs pre-treatment to remove the impurities [112]. Furthermore, there is a reduced occurrence of sintering in the treated limestone even after 100 cycles when compared to the initially treated limestone, as illustrated in Fig. 6(j) and (i), respectively.

4.1.1.5. Gluconic acid. Gluconic acid (GA) also exhibits a higher initial CO_2 capture capacity than unmodified limestone but has low stability where the CO_2 capture capacity drops to approximately 0.3 g CO_2/g sorbent from 0.625 g CO_2/g sorbent after 10 cycles [113]. The high initial CO_2 capture capacity is due to relative porous sheet like structure with small-sized grains, as shown in Fig. 6(a). The low CO_2 capture capacity after 10 cycles is attributed to the compact structure and shifting of the general pore size towards larger pores as shown in Fig. 6(b), which are not beneficial in CO_2 capture.

4.1.1.6. Tartaric acid. Hu et al., 2016 [109] investigated the effect of FA, AA, PrA, citric acid (CA), oxalic acid (OA), lactic acid (LA), malic acid (MA), and tartaric acid (TA) at a calcination temperature of 900 °C. TA exhibits the most effective carbonation conversions than other acids because it shows good anti-sintering properties which prevents the aggregation of grains, resulting in higher specific surface area at any operating conditions, as shown in Fig. 6(e) and (f). However, this study recommends introducing hydration treatment between two cycles for the modified sorbent. The summary of acid modifications for limestone is included in Table 5.

4.1.1.7. Summary of acid-modified limestone. Acid modifications were found to benefit the CO_2 capture capacity of the limestone due to its ability to exhibit higher surface area and pore volume. The improvement of CO_2 capture capacity by acid modification promotes the more active CaO, resulting in high CO_2 capture capacity. The certain range of surface area of acid-modified limestone ranges from 2.0 m^2/g to 18.0 m^2/g depending on the various limestone and acids. Meanwhile, the pore volume ranges from 0.007 cm^3/g to 0.200 cm^3/g to exhibit high CO_2 capture capacity.

Even though surface area and pore volume affect the CO_2 capture capacity, the amount of micropores (less than 2 nm) and mesopores (between 2 nm and 100 nm) can also affect the CO_2 capture capacity. The surface area, and pore volume of the acid-modified limestone depend on the pore size distribution, which has ranges of 1.8–4.6 nm and 18–155 nm, respectively. High amounts of micropores and mesopores are needed to exhibit high CO_2 capture capacity. Moreover, the formation of calcium formate demonstrates low surface area and pore volume but can exhibit high CO_2 capture capacity. The formation of calcium acetate exhibits better CO_2 capture capacity than calcium carbonate. Thus, acid modification can produce the formation of other calcium than calcium carbonate that enhances the CO_2 capture capacity of CaO sorbent. Moreover, TA is found to demonstrate CO_2 capture capacity more than other organic acids.

4.1.2. Dopants of limestone

Dopants are introduced into limestone to enhance CO_2 capture capacity and stability. The primary function of dopants is to modify the properties of limestone, improving reactivity and anti-sintering properties. Various dopants have been used in the modification of

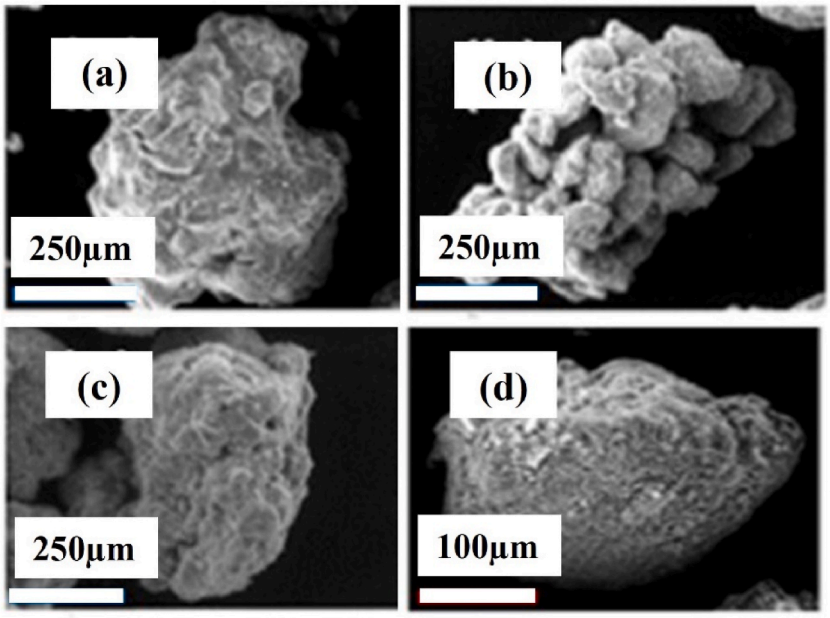

Fig. 7. SEM images of aluminate cement modified limestone (a) As-it-is (b) As-it-is first cycle (c) doped seawater (d) doped seawater 20 cycles (Reproduced from Morona et al., 2019 [119].

limestone, including salt solutions, seawater and inert materials.

4.1.2.1. Salt solution. Salt solution is a dopant material that can be used to enhance the CO_2 capture capacity of sorbents. Salt solutions such as potassium chloride (KCl) and potassium carbonate (K_2CO_3) [115] at different concentrations of 0.5 M and 0.05 M was doped for two different types of limestone. The results showed that 0.5 M KCl demonstrated high reactivity of long-term and low deactivation rate using Imeco limestone. However, it exhibited low initial reactivity because doping was restricted to the surface and not incorporated into the particle. Thus, potassium carbonate can be applied to reduce the attrition rate due to the agglomeration of the sorbent. However, Imeco limestone doped with K_2CO_3 exhibited poor reactivity at any concentration due to its high friability. This study contradicts with Xu et al. (2023) [116], where low amounts of K_2CO_3 (0.5 mol ratio) improved the CO_2 capture capacity at 0.55 g CO_2/g sorbent. A pore volume between 20 and 80 nm was found, indicating that high CO_2 capture capacity can be achieved through the doping of K_2CO_3.

Furthermore, the introduction of alkali salt dopants, such as KCl and sodium chloride (NaCl), improved the carbonation conversion of the $CaCO_3$ sorbent. This enhancement is attributed to the presence of K cations and Na cations in conjunction with Cl anions [117]. Whilst the Cl anion has the effect of retarding sintering, it simultaneously led to a decrease in carbonation conversion. However, the collaborative effect of K^+, Na^+ and Cl^- ions synergistically promoted the overall carbonation conversion of the $CaCO_3$ sorbent. Moreover, at carbonation temperatures exceeding 650 °C, NaCl formed a thin molten layer that covered the surface of CaO. This coating enhanced the transportability of CO_2 within the modified sorbent, leading to a considerable improvement in the carbonation ability during repeated CaL cycles [118].

4.1.2.2. Seawater. Seawater was also doped to the limestone to exhibit high CO_2 capture capacity. However, seawater-doped aluminate cement-modified limestone behaved poorly compared with undoped aluminate cement-modified limestone. This can be attributed to the lower presence of macropores in the undoped version, as depicted in Fig. 7(a) and (b). The decrease in macropores serves to mitigate surface area loss, thereby contributing to an improved CO_2 capture capacity. Meanwhile, doping causes the formation of eutectic mixtures from the melting of limestone and aluminate cement at different seawater concentrations, which leads to the formation of a flat surface at grain, indicating the eutectic melt to plug the macropores hindering the CO_2 adsorption, as shown in Fig. 7(c) and (d) [119]. The high CO_2 capture capacity of seawater-doped limestone can be achieved at relatively low doping concentration However, seawater-doped limestone improves the CO_2 capture capacity of limestone at low doping concentrations of 2.6×10^{-4} g [Na^+]/g [original limestone] and 4.7×10^{-4} g [Cl^-]/g [original limestone] [120]. Moreover, reducing the mass ratio of sea salt exhibits a high CO_2 capture capacity, i.e. 0.58 g CO_2/g sorbent, but decreases rapidly after 20 cycles [121].

4.1.2.3. Inert materials. Aluminium oxide, Al_2O_3–doped limestone was used to achieve the highest CO_2 capture capacity [122]. The composition of 90:10 of calcium acetate and aluminium nitrate using the hard templating method with absorbent cotton as template exhibited the highest CO_2 capture capacity amongst other compositions due to the hollow microtubular structure produced. This resulted in a reduction in markup flow, which is 34% lower than limestone when used inside the twin fixed bed reactors [123]. Then,

Table 6
Dopants.

Type of dopants	Composition	Powder size	Type of reactors	Process condition		Cycles	Sorption Performance (g CO_2/g sorbent)		Ref
				Carbonation	Calcination		Initial	Final	
Salt solution (KCl, K_2CO_3)	0.5 M	500–710 μm	Fluidised Bed	At 700 °C, for 10 min, under 15 vol % CO_2/85 vol% N_2	At 900 °C, for 10 min, under 100 vol% CO_2	10	0.42 g CO_2/g sorbent	0.25 g CO_2/g sorbent	[115]
Dope: Seawater (Natural, Pure) Binder: Calcium aluminate cement	10%	300–500 μm	TGA	At 650 °C, for 15 min, under 15 vol % CO_2/85 vol% N_2	At 850 °C, for 3 min, under 100 vol% N_2	20	70% Conversion	27% Conversion	[119]
Alumina, Al_2O_3 hard templating	90:10	–	Twin fixed-bed	At 700 °C, for 20 min, under 20 vol % CO_2/80 vol% N_2	At 850 °C, for 10 min, under 100 vol% N_2	30	0.63 g CO_2/g sorbent	0.58 g CO_2/g sorbent	[122]
Calcium aluminate	–	50 nm	TGA	At 650 °C, for 30 min, under 15 vol % CO_2/85 vol% N_2	At 850 °C, for 10 min, under 100 vol% N_2	15	0.47 g CO_2/g sorbent	0.23 g CO_2/g sorbent	[123]
Alumina, Al_2O_3	60:40	125–250 μm	Fixed bed	At 700 °C, for 3–8 min, under 25 vol % CO_2/75 vol% Air	At 930 °C, for 15 min, under 80 vol % CO_2/20 vol% Air	10	77% Conversion	25% Conversion	[124]
Zinc oxide, ZnO	–	N/A	TGA	At 600 °C, for 10 min, under 100 vol % CO_2	At 800 °C, for 10 min, under 100 vol% Ar	100	82% Conversion	38% Conversion	[125]
Zirconium oxide, ZrO_2	95:5	160 μm	TGA	At 850 °C, for 5 min, under 100 vol % CO_2	At 9850 °C, for 5 min, under 100 vol% CO_2	20	78% Conversion	50% Conversion	[126]
Cerium Oxide, CeO	90:10	–	Four fixed-bed	At 700 °C, for 20 min, under 15 vol % CO_2/85 vol% N_2	At 800 °C, for 10 min, under 5 vol % CO_2/95 vol% H_2O	10	0.71 g CO_2/g sorbent	0.67 g CO_2/g sorbent	[127]

the addition of calcium aluminate cement in limestone produced mayenite ($Ca_{12}Al_{14}O_{33}$), which acted as thermally stable and mechanical support that reduced the sintering effect. However, nano limestone doped with calcium aluminate demonstrated the highest CO_2 capture capacity and stability over long cycles owing to more extensive interface contact with cement where numerous $Ca_{12}Al_{14}O_{33}$, is formed. Meanwhile, Teixeira et al. (2022) [124] found that adding less than 38% of Al_2O_3 produced more tricalcium aluminate ($Ca_3Al_2O_6$), than calcium aluminate ($CaAl_2O_4$). The presence of $Ca_3Al_2O_6$ and $CaAl_2O_4$ reduces the available CaO for CO_2 capture capacity. However, the substantial quantity of $CaAl_2O_4$ serves as structural support, enhancing the mechanical resistance of the sorbent. This improvement in mechanical strength contributes to an overall enhancement in the CO_2 capture capacity of the sorbent. The composition of 60:40 of limestone and Al_2O_3 can produce high $CaAl_2O_4$, which exhibits the highest carbonation conversion due to the yield of mesopores and provides active sites for CO_2 adsorption.

Zinc-oxide, ZnO–doped limestone [125] demonstrates lower carbonation conversion, i.e. approximately 82% compared with the undoped one, which demonstrates 90% during the first 20 cycles but remains higher afterwards (100 cycles). The high reaction is due to the anti-sintering effect, effective Zener pinning force, and self-reactivation phenomenon. Meanwhile, adding zirconium dioxide (ZrO_2) in limestone increased the carbonation conversion from 19% to 40% after 20 cycles due to the high Tammann temperature of ZrO_2 that prevents sintering during calcination [126]. However, adding ZrO_2 demonstrates lower initial carbonation conversion than undoped limestone during the first cycle but remains stable afterwards.

Then, adding cerium (IV) oxide, CeO_2 exhibits high CO_2 capture capacity (0.72 g CO_2/g sorbent), which slowly decreases to 0.65 CO_2/g sorbent after 10 cycles due to its anti-sintering properties [127]. In addition to high CO_2 capture capacity, doped CeO maintains the stability of limestone after several cycles. The summary of limestone reinforcement is included in Table 6.

4.1.2.4. Summary of doped limestone. In summary, the addition of dopants to limestone enhances stability but often leads to a lower initial CO_2 capture during the first cycle. These dopants activate anti-sintering properties that effectively mitigate the sintering of regenerated CaO during calcination, even under harsh conditions and temperatures exceeding 900 °C in practical applications.

However, limestone modified with Al_2O_3, resulting in $Ca_3Al_2O_6$, exhibits an inferior CO_2 capture capacity. Higher levels of Al_2O_3 in limestone modification promote the formation of a larger volume of pores smaller than 10 nm, contributing to the reduced CO_2 capture capacity. The optimal pore size for effective CO_2 capture capacity falls between 20 and 100 nm, with an increased number of pores within this range correlating with higher CO_2 capture capacity. For example, CeO–doped limestone demonstrates a CO_2 capture capacity of 0.72 g CO_2/g sorbent, with the pore size ranging from 10 to 100 nm. This CO_2 capture capacity is almost near the theoretical maximum of 0.786 g CO_2/g sorbent.

Whilst dopants have the potential to enhance CO_2 capture capacity and resist sintering effects, careful consideration of the

associated costs is essential because it can considerably affect operational expenses.

4.1.3. Treatment of limestone

Limestone treatments, such as hydration, hydrogen chloride (HCl), and thermal treatment, can be used to increase the sorbent CO_2 capture at high temperatures, which may be a cost-effective approach.

4.1.3.1. Hydration. Introducing steam during the carbonation stage increases the CO_2 capture capacity by 15% more than normal carbonation due to the decrease in the fraction of fines lost by elutriation, indicating the sorbent resistance towards attrition [128]. In addition, the presence of steam can increase the diffusion of CO_2 through the sorbent pores [129,130].

4.1.3.2. HCl treatment. Meanwhile, HCl treatment was administered during the carbonation step in some cycles; after third carbonation is beneficial to increase the carbonation conversion due to the formation of calcium hydroxychloride (CaClOH) [131]. The HCl addition in the previous three cycles demonstrated the highest initial carbonation conversion and the most stable amongst other cycles at a calcination temperature of 850 °C. However, the result contradicts the study by Symnonds et al.(2021) [132] where HCl demonstrated low carbonation conversion at 870 °C due to the formation of calcium chloride ($CaCl_2$) onto the surface, causing an increase in CO_2 diffusion resistance. Moreover, the contradiction is probably due to the number of HCl additions during the carbonation stages. Nevertheless, carbonation conversion increases with the presence of HCl and steam, where the $CaCl_2$ decomposes to CaO during this calcination process. However, the presence of HCl can lead to potential corrosion and hence, equipment failure issues.

4.1.3.3. Thermal treatment. During the thermal treatment, the pelletised sorbents consisting of limestone and calcium aluminate-based cement were heated in an in-situ reactor at 900 °C in flowing gases [133]. Initially, the thermal treatment exhibited low initial CO_2 capture capacity but eventually displayed high stability after the third cycle, especially at 7.5 °C/min, suggesting that the thermal treatment had stabilised the pellets. Moreover, increasing the percentage of steam to the sorbent increases CO_2 capture, especially at 30% of steam.

Moreover, the thermal treatment at 1100 °C demonstrated the highest CO_2 capture capacity compared with that at 900 °C, 1000 °C, and 1200 °C [134]. However, the degradation trends remained unchanged over the carbonation/calcination cycles. Adding MgO through hydration maintained the stability of limestone treated at 1100 °C but with a lower initial CO_2 capture capacity than that without MgO. However, limestone treated at 1100 °C demonstrated 83.9% of the initial value after reactivation in humid air. Thus, the treatment of limestone, either using steam, HCl, and thermal treatment, can increase the CO_2 capture and improve the stability of the sorbent.

4.1.3.4. Summary of treated limestone. Hydration or the steam treatment of limestone has been proven effective in enhancing CO_2 capture capacity, particularly when steam treatment is applied in the calciner reactor or in the calciner and carbonation reactors. The microporosity of the sorbent plays a crucial role in determining accessibility and reactivity, with the lowest microporosity observed without steam treatment (<1 mm^3/g) and increased microporosity with steam treatment (~ 5 mm^3/g).

The CO_2 capture capacity achieved with steam treatment in the calciner and carbonator reaches 0.191 g CO_2/g sorbent but deactivates to 0.078 g CO_2/g sorbent after four cycles. Notably, steam treatment inside the carbonator alone demonstrates a larger CO_2 capture capacity than treatment without steam, which is attributed to the catalytic role of steam that enhances CO_2 diffusion. Although the CO_2 capture capacity remains relatively lower than the theoretical capacity of CaO sorbent, the introduction of steam still results in a slight improvement.

The addition of water (H_2O) during the process contributes to the hardening of particle surfaces, resulting in a decrease in attrition rate. Furthermore, discontinuously adding hydrochloric acid (HCl) is only effective during the early seven cycles in the carbonation step, with lesser HCl addition demonstrating better CO_2 capture capacity, especially at the third cycle during carbonation.

Moreover, thermal pre-treatment enhances the sintering effect of the CaO sorbent, influencing its overall performance in CO_2 capture applications. These findings collectively underscore the importance of optimising treatment methods to maximise the efficiency and sustainability of CO_2 capture processes.

4.2. Dolomite

The enhancement of dolomite is needed to increase the regenerability of CaO sorbents, increase the CO_2 capture capacity and improve the performance of CaO sorbents, leading to a reduction in operational cost in large-scale applications. Therefore, several studies investigating the enhancement of dolomite have been conducted in the past few years (e.g. acid modifications, doping and treatment).

4.2.1. Acid modifications of dolomite

Acid modification is found to increase the surface area of CaO sorbent, thus increasing the CO_2 capture capacity. Organic acids are widely used to improve the CO_2 capture capacity of CaO sorbent due to the low cost. However, different acids demonstrate different CO_2 capture capacity.

4.2.1.1. Acetic acid. AA can improve the properties of sorbents. However, diluted AA under high CO_2 partial pressure, 70% of CO_2 during the calcination process does not improve the capture capacity of dolomite and only demonstrates high residual capture capacity when recarbonation is introduced [110]. The MgO grains that presumably mitigate the aggregation and sintering of the CaO grains cannot resist the degradation with AA treatment under high CO_2 partial pressure. Nevertheless, AA improves the CO_2 capture capacity more than untreated dolomite at a calcination temperature of 920 °C under a high CO_2 concentration of 80 vol% [135]. However, AA is pricey; thus, waste AA, such as acetone, can be replaced.

4.2.1.2. Citric acid. Dolomite treated with carbon coating using CA at a high calcination temperature (>800 °C) demonstrates three times higher CO_2 capture capacity than unmodified limestone, especially under a dual calcination environment where two gases were used, i.e. air and N_2 [136]. The porous structure is preserved after 20 cycles because in situ carbon prevents crystallite agglomeration. Furthermore, the Mg-doped calcite phase hinders the de-mixing of Ca and magnesium (Mg), which improves the anti-sintering of sorbent [113].

4.2.1.3. Gluconic acid. The addition of GA slightly improves the initial CO_2 capture capacity and exhibits a similar trend of cyclic CO_2 capture performance of untreated dolomite under a realistic condition due to the preserved high porosity after 10 cycles despite a large grain size. Moreover, the presence of a homogeneous mixture of Ca–Mg reduces the segregation of MgO during the carbonation–calcination cycles.

4.2.1.4. Propionic acid. Furthermore, dolomite modified with PrA has a lower initial CO_2 capture capacity than undoped dolomite but exhibits a stable CO_2 capture capacity [137]. In conclusion, dolomite acid modification improves the sorbent's stability but shows no improvement in terms of initial capture capacity.

4.3. Summary of acid-modified dolomite

The introduction of acid to dolomite in the modification process results in an augmentation of surface area and pore volume of the sorbent. This enhancement yields an impressive surface area exceeding 20.0 m^2/g and a substantial pore volume exceeding 0.080 cm^3/g. Notably, acid-modified dolomite surpasses limestone in surface area because the raw dolomite alone already possesses a surface area of 18.4 m^2/g and a pore volume of 0.076 cm^3/g. Using modified acid, low CO_2 capture capacity is obtained using PrA from 0.45 g CO_2/g sorbent (raw dolomite) to 0.39 (g CO_2/g sorbent). However, it can slightly maintain the CO_2 capture capacity at 30 cycles. Then, the abundance nano size of the modified sorbent is obtained, ranging between 40 and 50 nm. In summary, acid modification of dolomite does give minimal impact on improvement of CO_2 capture capacity.

4.3.1. Dopants of dolomite

Dopants are used to improve the reactivity and anti-sintering properties for dolomite in CaL. Various dopants have been used in the modification of dolomite, including alkali metal salt and inert materials.

4.3.1.1. Alkali metal salt. Alkali metal salt such as sodium bromide (NaBr) were doped to the limestone but showed no improvement in CO_2 capture capacity compared with NaBr–doped limestone but was able to maintain cyclability in the long-term [138]. Even though dolomite naturally consists of MgO, an anti-sintering material, the presence of MgO in calcined dolomite has no considerable effect on NaBr–doped dolomite. Moreover, the degradation trend of CaO precursors doped with NaBr contributes to the production of alkali metal salts that reduce the sorbent's melting point temperature and accelerate the sintering effect, which in turn decrease the CO_2 capture capacity.

However, the presence of NaBr enhances the SO_2 capture capacity during the sulphation condition and can maintain the CO_2 capture capacity at a high presence of SO_2. The stability of the NaBr-modified dolomite is contributed by larger fractal dimensions (D) than unmodified sorbent after 10 cycles [139]. Fractal dimensions refer to the roughness of sorbent surface where the high fractal dimension has high CO_2 capture capacity. Alkali metal salts, such as sodium carbonate (Na_2CO_3) and K_2CO_3, which doped dolomite at 0.05 M ratio, displayed lower CO_2 capture capacity than undoped dolomite [79]. However, the lithium carbonate, Li_2CO_3–doped dolomite at a molar ratio of 0.05 exhibited a similar trend of CO_2 capture capacity to undoped dolomite, which is attributed to the inhibition effect of the MgO skeleton on sintering. In conclusion, alkali metal salt–doped dolomite does not show any improvement of CO_2 capture capacity to the dolomite.

4.3.1.2. Inert materials. Bai et al. (2022) [137] doped the dolomite with Fe1–Mn0.5 but it exhibited a lower initial CO_2 capture capacity but better stability than undoped dolomite. This binary doping of Fe and Mn ions is CaO-based composite. However, the stability of acid-modified dolomite is better than acid-modified doped Fe–Mn, even at 30 cycles.

Thus, doping cannot increase the CO_2 capture capacity but only improves the stability of dolomite. Moreover, the extrusion-spheronisation technique can be used during the preparation of dolomite-derived composite pellets, which can display good mechanical properties such as ability to resist mechanical stress and thermal shock.

4.4. Summary of doped dolomite

The introduction of alkali metal salts has a notable effect on dolomite, reducing its specific surface area from 29.5 m^2/g to 3.5 m^2/g and decreasing pore volume from 0.195 cm^3/g to 0.020 cm^3/g. Pores larger than 20 nm almost disappear, and causes a low CO_2 capture capacity. However, dolomite modified with lithium carbonate maintains a comparable CO_2 capture capacity to unmodified dolomite. This outcome suggests that different alkali carbonates exert varying effects on CO_2 capture capacity when specific surface area and pore volume are low.

Doping with Fe and Mn results in the formation of calcium magnesium iron oxide ($Ca_2MgFe_2O_6$), $Ca_4Mn_3O_{10}$ and ferric oxide (Fe_2O_3) at increasing dopant concentrations. This doping leads to a decrease in CO_2 capture capacity to 0.387 g CO_2/g sorbent due to the generation of the complex Ca–Mn–Fe. Furthermore, an increase in pore diameter, particularly in the range of 1–3 nm, decreases CO_2 capture capacity, especially when using NaBr–doped dolomite. Despite this, the material manages to sustain CO_2 capture capacity after 50 cycles. Hence, dopants for dolomite may not enhance CO_2 capture capacity but contribute to maintaining stability over carbonation/calcination cycles.

4.4.1. Treatment of dolomite

Dolomite treatments are used to enhance the sorbent CO_2 capture capacity, such as activation and reactivation. Reactivation of spent sorbent can reduce the replacement of new CaO sorbent, which may be a cost-effective approach.

4.4.1.1. Activation. Sun et al.(2018) [140] performed wet mechanical activation of the dolomite and found that prolonging the ball milling duration is beneficial to improving the cyclic CO_2 capture capability of wet ball milled dolomite. It is mainly attributed to the reduced particle size and maintained porous microstructure, which promotes the accessibility of CO_2 to the interior, free CaO. Moreover, calcined dolomite with ball milled treatment enhances the sorption capacity and stability of the sorbent [67]. The samples show no sintering effect due to the ball mill process preventing CaO – MgO separation. Despite this, only a few studies investigated the CO_2 capture capacity of CaO sorbent under realistic conditions (more than 900 °C) because the calcination temperature of this study is 800 °C.

4.4.1.2. Reactivation. Moreover, the degradation of sorbent after several carbonation–calcination cycles initiate the replacement of CaO sorbent in the CaL cycle. Therefore, introducing the reactivation of spent sorbent reduces the sorbent replacement in the CaL cycle because the spent sorbent can be recycled in CaL. Ball milling and hydration are the reactivation methods for spent sorbent after CaL looping. Ball milling can crush the spent sorbent into micro-particles, which must be controlled for milling time. Longer milling time decreases crystallite and particle size, but more defects, such as particle agglomeration, are found than shorter milling time. Thus, controlling the milling time to control the particle size would be useful for the industrial reactor system. Su et al. (2019) [71] proposed the use of ball milling–assisted carbonation conversion reactivation (BMCR) in reactivating the spent dolomite. This method uses dry ice and ice and mixed with the dolomite inside stainless-steel jars prior to planetary ball milling. The CO_2 capture capacity of reactivation sorbents is almost like fresh dolomite, and it exhibits 2.5 times higher than spent sorbent. Meanwhile, reactivation using hydration shows superior activity than ball milling shows but inferior of BMCR. Thus, BMCR is a good method for reactivation because it can offer nanocrystalline oxide, and the surface morphology is slightly compressed and dense.

In addition to pre-treatment or activation of sorbents, spent sorbents can be reactivated to improve the CO_2 capture capacity. The reactivation can decrease the amount of sorbent replacement during the CaL operation and hence reduce the operational cost.

4.5. Summary of treated dolomite

Wet ball milling has been proven effective in enhancing the BET surface area of dolomite, elevating it from 22.0 m^2/g to 23.4 m^2/g, along with a notable increase in pore volume from 0.191 cm^3/g to 0.239 cm^3/g. This process has also successfully reduced the particle size of dolomite from 88.1 μm to 6.57 μm after 120 min of milling.

Furthermore, reactivating spent sorbent through ball milling, utilising a combination of water (H_2O) and dry ice, has yielded a specific surface area of 22.2 m^2/g, with observed pore diameters around 2–3 nm.

Notably, the analysis of the spent sorbent indicates that only the micropores in the range of 2–3 nm considerably affects CO_2 capture capacity. This result highlights the pivotal role of these specific micropore characteristics in determining the sorbent's efficacy in capturing CO_2. Understanding and optimising micropore properties emerge as crucial factors for achieving efficient and effective CO_2 capture processes. The reactivation of spent sorbent through such methods holds promise in reducing the need for frequent CaO sorbent replacements during operational use.

4.6. Biogenesis calcium waste

The type of biogenesis of calcium waste exhibits different CO_2 capture capacities. Clam shells are found to be the most stable CaO sorbents after eight cycles; they keep high residual carrying activity and has lower content of trace elements (i.e. K, Si, Al, Mg, S, Zr, Sr, and P) in the structure compared with cockle shells, crab shells, cuttlefish shells, oyster shells and scallop shells [73]. Furthermore, all the samples show a CO_2 capture capacity of less than 0.3 g CO_2/g sorbent at the first cycle. Modifications, such as acid modification, doping and pretreatment, must be performed to increase the CO_2 capture.

4.6.1. Acid modification of biogenesis calcium waste

According to Iyer and Fan (2010) [141], adding an aqueous acid solution to the biogenesis of calcium waste can remove the collagen-containing membranes that prevent CO_2 capture. Thus, many studies were found using acids during biogenesis calcium waste modification.

4.6.1.1. Acetic acid. For AA, the eggshells display a CaO conversion higher than unmodified eggshells after 20 cycles due to increasing the textural feature of sorbents, e.g. porosity that leads to an increase in CO_2 capture capacity [142]. In addition, the high acidity of eggshells causes less particle adhesion that prevents pore blocking, hence increasing CO_2 diffusion.

Nawar (2021) [143] studied different types of acids (CA, FA, AA, PrA, LA, CA monohydrates, and MA) with the composition of 10% from the waste eggshells. The AA, CA, and FA exhibited the maximum carbonation conversion with 54.39%, 55%, and 55.5%, respectively, after 20 cycles because acid modifications altered the surface structure, which decreased the sintering effect after multiple cycles. In addition, pre-treatment of quail eggshells using AA exhibited higher carbonation conversion after 19 cycles than untreated quail eggshells [74]. Thus, acid modification positively affects CO_2 capture capacity and CaO conversion. However, based on previous studies, large amounts of acid are needed to enhance the CaO conversion and CO_2 capture capacity of the calcium waste as a CaO sorbent. Based on stoichiometric equation, 2 mol of AA is needed for 1 mol of $CaCO_3$ hence, increasing the operational cost.

4.6.1.2. Glycine. Glycine-modified eggshell demonstrates a high surface area of 10.66 m^2/g and pore volume of 0.0551 ml/g, where rich micropores were found in the range of 0–2 nm [144]. The rapid chemical reaction stage of glycine-modified eggshell is longer than that of unmodified sorbent, indicating better carbonation conversion, which can absorb more CO_2.

4.7. Summary of acid-modified biogenesis calcium waste

The surface area of biogenesis calcium waste undergoes a substantial increase from 0.4 m^2/g to 10.3 m^2/g through acid modification. This augmentation is attributed to the formation of pores during the decomposition of organic salts to oxide. However, despite this enhancement, the maximum CO_2 capture capacity achieved with acid modifications stands at only 0.48 g CO_2/g sorbent when using AA-treated eggshells. Compared with the theoretical value of 0.786 g CO_2/g sorbent, the acid-modified biogenesis calcium waste shows only marginal improvement in CO_2 capture capacity.

4.7.1. Dopants of biogenesis calcium waste

In addition to acid modifications, dopants can increase the CO_2 capture capacity and stability of the biogenesis of calcium waste.

4.7.1.1. Inert materials. Modification of the eggshells and marble dust using lanthanum (La), magnesium (Mg), and aluminium (Al) as inert materials at different synthesisation methods, such as dry mixing, wet mixing and sol–gel process, demonstrates different carbonation conversion or CO_2 capture capacity [145]. Marble dust exhibits higher carbonation conversion than eggshells using sol–gel and dry mixing as synthesisation methods. However, dry mixing exhibits a low carbonation conversion due to the non-existence of transient phase transformation, such as $Ca_{12}Al_{14}O_{33}$ or $Ca_3Al_2O_6$, because no mixed phases occurred. Only phases of CaO, and Al_2O_3, La_2O_3 or MgO exist when analysed using X-ray crystallography (XRD). Meanwhile, the sol–gel process demonstrates the highest carbonation conversion of marble dust with La as the supporting material. Nevertheless, the wet method can easily be scaled up at low cost with less time consumption. Furthermore, high stability can be achieved using wet mixing for marble dust, and the highest carbonation conversion of eggshell can be obtained using doped La. Furthermore, Huang et al.(2022) [146] doped the eggshells with MgO at different molar ratios. The ratio of 80:20 of eggshells and MgO shows the best CO_2 capture capacity and has highest stability amongst the other compositions due to the 3D hierarchically ordered structures that produce less agglomeration, thus hindering the sintering.

Imani et al. (2023) [147] studied the potential of eggshells with silica (SiO_2) in increasing the CO_2 capture capacity. The presence of 7.5% SiO_2 exhibits higher carbonation conversion even at different preparation methods. Furthermore, Shan et al. (2016) [148] doped the eggshells with bauxite tailings (BT); results showed 10% BT demonstrate >55% conversion after 40 cycles. The formation of $Ca_{12}Al_{14}O_{33}$ is favourable for increasing the cyclability of CaO sorbents [149].

Zr-doped eggshells exhibited outstanding performance, maintaining a carbonation conversion rate of approximately 88% throughout 20 cycles [150]. The creation of calcium zirconate ($CaZrO_3$) plays a pivotal role in inhibiting the growth of CaO particles, effectively slowing down the sintering–agglomeration process by separating $CaO/CaCO_3$ particles [150,151].

4.7.1.2. Surfactants. In addition to inert materials, surfactants were used to increase the CO_2 capture capacity. Hsieh et al. (2021) [80] altered the eggshells with surfactants cetyltrimethylammonium bromide (CTAB), sodium dodecyl sulfate (SDS) and lauryl dimethyl betaine (BS-12) and amino–based polymers tris(hydroxymethyl)aminomethane (Tris), Polyethylenimine (PEI), and polydopamine (PDA). The alteration with surfactant does not increase the CO_2 capture capacity of $Ca(OH)_2$ from eggshells because positively charged surfactants on the surface of Ca^{2+} ions attract OH- ions and precipitate with Ca^{2+} ions when using CTAB. For the SDS, electrostatic repulsive forces between the negatively charged entities cause OH^- ions to be away from the Ca^{2+} ions [152]. However, the lowest deactivation rate was achieved when using lauryl dimethyl betaine BS because it has a spherical shape and porous structure that allows the CO_2 to react more with CaO. However, eggshells treated with amino-based polymers exhibit the highest CO_2 capture capacity when using PDA as supporting material. This contributes to the polymeric films that formed and likely to be thermally pyrolyzed at high

calcination temperature which caused the production of microporous channels. However, the CO_2 capture capacity of PDA treated after 10 cycles was 0.40 g CO_2/g sorbent, which is lower than the theoretical CO_2 capture capacity of $CaCO_3$, which is 0.786 g CO_2/g sorbent; thus, the replacement of sorbent becomes a concern. Moreover, different types of CaO sorbent precursors were studied in this work, and results showed that the calcination of $Ca(OH)_2$ from eggshells exhibits three times higher initial CO_2 capture capacity (from 0.63 g CO_2/g sorbent at first cycle and reduce to 0.25 g CO_2/g sorbent after 10 cycles) than direct eggshell calcination and $CaCO_3$ obtained from eggshells.

4.8. Summary of doped biogenesis calcium waste

Despite the ability of Al-doped biogenesis calcium waste to produce mayenite, it exhibits low CO_2 capture capacity due to the formation of mayenite on the surface of eggshells. By contrast, La demonstrates a higher CO_2 capture capacity, reaching 70.85% carbonation conversion, especially when synthesised using sol–gel combustion synthesis. In contrast to Al_2O_3, La_2O_3 does not show mixed phases with CaO.

The modification using surfactants results in a decrease in surface area to 62.56 m^2/g using PDA. However, it simultaneously exhibits a higher CO_2 capture capacity of 0.62 g CO_2/g sorbent. This enhancement is attributed to the formation of a polymeric film on the sorbent's surface.

In the case of chicken eggshells, the highly porous structure with a large mesopore volume of 0.15–0.20 cm^3/g and a pore size of 2–10 nm contributes to a CO_2 capture capacity of 0.52 g CO_2/g sorbent. This emphasises that whether a dopant can produce mixed phases and the resulting CO_2 capture capacity is not solely dependent on surface area but also involves intricate material characteristics.

4.8.1. Treatment of biogenesis calcium waste

Biogenesis calcium waste treatments, such as thermal treatment can improve the CO_2 capture capacity.

4.8.1.1. Thermal treatment. Previous research has indicated that the sorption capacity or CO_2 capture capacity of calcined eggshells are highly encouraging compared with raw eggshells [75]. The phase transformation of duck eggshells from $CaCO_3$ to CaO occurs at a temperature above 700 °C [153]. Normally, phase transformation occurs at a temperature of 825 °C, which requires substantial heat to break the bond between $CaCO_3$ to become CaO. The phase transformation indicates the amount of heat needed in calcination. Moreover, the thermal pre-treatment method plays an important role in the amount of heat needed during calcination in CaL. The thermal pre-treatment of the waste shell (oyster) using microwave requires lower energy input and lower rank of heat resistance required for the thermal apparatus compared with sorbent produced by conventional calcination [154]. Using microwave-assisted 900 W, which indicates a temperature of around 621 °C, the mass loss increases from 15.78% to 40.64%, where the maximum theoretical mass loss of waste oyster shell calcination should be more than 39.05%. However, conventional calcination requires a temperature of approximately 900 °C to lose mass at 43.82%. The mass loss is where the $CaCO_3$ becomes CaO. Nevertheless, the temperature inside the waste oyster shells could be substantially higher than measured during microwave heating. Thus, Troya et al. (2020) [155] investigated different pre-treatments such as ball milling and thermal treatment, on snail shells and eggshells. For the eggshells, the result contradicts with previous research [156] because untreated eggshells shows best CO_2 capture capacity than ball milled and pre calcined for 4 h at 850 °C. The crystal structure affects the CO_2 capture capacity of the sorbent, which is why an aragonite structure exhibits better performance than a crystal structure due to a less dense packed crystal lattice. Meanwhile, the pre calcined snail shells exhibit highest carbonation conversion 11.2% and decrease to 5.2% after 20 cycles. For the comparison, the eggshells demonstrate higher carbonation conversion than snail shells. The high presence of Na_2O and K_2O in snail shells as impurities promote the sintering during the carbonation–calcination cycles, hence reducing the carbonation conversion. During high–temperature calcination, the Na^+ ions are incorporated into the crystal structure of CaO and cause the lattice defect. This defect enhances the sintering that is not favourable in CO_2 capture capacity [157].

4.9. Summary of treated biogenesis calcium waste

Increasing the calcination temperature from 700 °C to 825 °C has been observed to enhance the surface area of eggshells in a nitrogen (N_2) environment, escalating it from 2.001 m^2/g to 10.063 cm^3/g. This increase in surface area creates more active sites, thereby positively affecting the CO_2 capture capacity of the sorbent. However, the average sizes of the sorbent at higher temperatures are larger due to the merging of smaller sizes and the growth of CaO grain size, which is attributed to sintering at elevated temperatures.

Conversely, calcination under static air has been found to decrease the specific surface area. Despite this decrease, the sorbent can maintain CO_2 capture capacity even after 20 cycles. This result suggests that under certain conditions, the decrease in surface area does not compromise the sorbent's effectiveness in capturing CO_2 over multiple cycles.

The chemical composition of the sorbent is identified as a critical factor in determining CO_2 capture capacity after thermal pre-treatment. Understanding and optimising the chemical composition become crucial considerations in tailoring the sorbent for efficient and sustainable CO_2 capture processes.

4.10. Industrial waste

Industrial waste such as CS, LM, BFS, and WMP demonstrate the decay in sorption capacity after several cycles in CaL. The improvement of industrial waste enhances the CO_2 capture at a low cost and reduces the makeup rate.

4.10.1. Acid modifications of industrial waste

Acid modifications of industrial waste, such as PrA and AA, are found to increase the surface area and pore volume of sorbent, which enhances the CO_2 capture capacity after several carbonation-calcination cycles.

4.10.1.1. Propionic acid. In acid modification, PrA is used in modifying the carbide slag and manages to improve the carbonation conversion by approximately 53.7% more than pure carbide slag after 20 cycles [158]. Then, pyroligneous acid-modified CS demonstrates carbonation conversion 2.8 times higher than limestone [159]. Thus, acid modification increases the pores and spaces between the grains of the sorbent, which enhances the diffusion of CO_2 into CaO sorbent. However, the initial CO_2 capture is lower than unmodified CS and limestone.

4.10.1.2. Acetic acid. Modified BFS with AA modification demonstrates the highest carbonation conversion, i.e. from 35% to 25%, after 20 cycles [160]. The formation of small rods after the AA treatment increases the surface area. Then, the presence of silica as impurities in sorbent after the acid modification provides thermal stability that can prevent the sintering effect, implying no or only a slight decrease in the CO_2 capture capacity of the sorbent [161]. Nawar et al. (2019) [105] studied the effect of various acids (AA, CA, FA, LA, L-MA, TA, OA, and PrA) with WMP and reported that PrA and AA exhibit higher carbonation conversion than other acids, demonstrating high stability. The highest carbonation conversion can be achieved by increasing the volume percentage of the acid solution. This causes changes in the pore structure, increasing the surface area of sorbent, hence increasing carbonation conversion. Even though the acid modification achieved the highest carbonation conversion and CO_2 capture capacity, using organic acids can increase the sorbent cost, thus increasing the operational cost of CaL.

4.11. Summary of acid-modified industrial waste

Industrial waste often contains impurities that can either enhance or diminish CO_2 capture capacity. The presence of alumina, for example, leads to the formation of calcium aluminate, which, unfortunately, reduces CO_2 capture capacity by removing active CaO during carbonation because calcium aluminate cannot effectively absorb CO_2. By contrast, the formation of calcium silicates in the presence of silica proves beneficial as it helps mitigate the sintering effect, providing thermal stability.

Elements, such as magnesium, iron, and titanium, are inert materials, contributing to the overall stability of the waste. However, when considering acid modification, the choice of acid becomes critical. Formic acid, for instance, reduces the surface area of WMP, thereby decreasing CO_2 capture capacity. By contrast, acetic acid and propionic acid are more favourable, resulting in a remarkable increase in CO_2 capture capacity. This increase is evident in the transition from 0.63 g CO_2/g sorbent in raw marble powder to 0.675 and 0.645 g CO_2/g sorbent, respectively, achieved by enhancing the surface area from 6.007 m^2/g to 31.39 m^2/g.

4.11.1. Dopants of industrial waste

In addition to acid modifications, dopants can increase the CO_2 capture capacity and stability of the industrial waste.

4.11.1.1. Inert materials. One of the dopants used to reinforce industrial waste is bauxite tailings (BT). Based on previous research, doped BT enhances the CO_2 capture capacity of CaO sorbents due to the formation of $Ca_{12}Al_{14}O_{33}$ [162]. However, LM doped with aluminium nitrate demonstrates higher carbonation conversion than LM doped with BT [162]. The development of the $Ca_{12}Al_{14}O_{33}$ phase in LM with aluminium nitrate proves that the $Ca_{12}Al_{14}O_{33}$ produces a stable framework inhibiting the inactivation of CaO during the carbonation/calcination cycles, and the release of CO_2 from $CaCO_3$ increases the pore channel, thus improving the sorption capacity. The inferiority of BT is because of impurity in BTs, such as Fe_2O_3 and TiO_2, which limits the reactivity of sorbent during carbonation.

Cai et al. (2022) [31] modified the CS with single and binary doping of MgO and ZrO_2. For the single doped, CS–MgO–7–3 has a high initial CO_2 capture capacity but has the lowest stability than CS–NiO–8–2 and CS–ZrO_2–9–1. Thus, the combination of CS–MgO–NiO or CS–MgO–ZrO_2 can counteract the disadvantages of MgO, NiO, and ZrO_2. The CS–MgO–ZrO_2 demonstrates a higher initial CO_2 capture capacity and stability than CS–MgO–NiO due to the formation of ZrO_2 and $CaZrO_3$, which prevents the growth of CaO grains during the carbonation/calcination cycles. The binary doped is foreseen to exhibit high stability under mild and severe calcination conditions. Ma et al. (2020) [163] doped the carbide slag with dolomite and manganese nitrate. This binary doping resulted in a slightly lower initial CO_2 capture capacity than CS–Mn, and CS–MgO doped but exhibits good stability after the 10 cycles. The binary doping was maintained from 0.56 g CO_2/g sorbent to 0.52 g CO_2/g sorbent after 10 cycles. The MgO acts as a skeleton to the CaO sorbent to reduce the sintering effect, whereas the manganese ion enhances the electron transfer between CaO and CO_2 [164]. The CO_2 capture capacity of CS–Mn was found to be inferior to CS–MgO due to Mn_2O_3, which consists of Mn^{3+} ions that are unstable due to intermediate valence. The formation of Mn_2O_3 comes from the decomposition of MnO_2 at a temperature above 535 °C. Thus, the optimal composition of Mn doping is required to maintain the CO_2 capture capacity, and the value is 0.75% according to Ca/Mn molar ratio. Moreover, the presence of 20% steam of 0.75% Mn doped to the CS–MgO exhibits high stability where the CO_2 capture capacity

is from 0.6 g CO_2/g sorbent to 0.59 g CO_2/g sorbent after 10 cycles. This result is attributed to the effect of MgO as a stabilizer and the synergetic effect of MnO_2 and steam.

Wang et al. (2022) [165] modified the carbide slag with binary doped Ni-doped and Al-doped, and Ni-doped and Mg-doped under the presence of steam. As a result, the Ni–CaO–$Ca_{12}Al_{14}O_{33}$ demonstrates a CO_2 capture capacity 2 times higher than Ni–CaO–MgO due to the formation of $Ca_{12}Al_{14}O_{33}$ that can prevent the sintering and aggravation of sorbent, hence producing the excellent framework. The improvement of $Ca_{12}Al_{14}O_{33}$ was also studied by Ma et al.(2019) [166] where the $Ca_{12}Al_{14}O_{33}$ improves the cyclic stability of CO_2 capture even at the severe calcination temperature where the CO_2 capture capacity is 0.29 g CO_2/g sorbent after 100 cycles, which is 80% higher than unmodified carbide slag.

Teixiera et al., 2019 [72] used WMP reinforced dolomite as Ca precursors. The carbonation conversion of WMP reinforced dolomite rapidly decreased at severe calcination conditions and slightly lower than using pure dolomite as CaO sorbent after 20 cycles. For the mild calcination condition, the CO_2 capture capacity of dolomite is higher than the combination of dolomite and WMP. In addition, the presence of MgO improved the stability of WMP after several cycles.

4.12. Summary of doped industrial waste

Incorporating inert materials such as magnesium oxide, nickel oxide, zirconium oxide, and aluminium oxide as dopants for industrial waste is a widespread practice. Although magnesium oxide initially enhances CO_2 capture capacity, its effectiveness diminishes after 20 cycles. Conversely, nickel oxide (NiO) and zirconium oxide (ZrO_2) showcase the ability to enhance the cyclic stability of industrial waste, particularly in the case of carbide slag. Notably, the application of binary dopants proves more effective than using single dopants.

In the context of aluminium oxide (Al_2O_3), the formation of the $Ca_{12}Al_{14}O_{33}$ phase is pivotal for establishing a stable framework that prevents the inactivation of CaO. This stabilisation considerably amplifies CO_2 adsorption. For lime mud, the addition of Al_2O_3 results in a substantial increase in surface area from 2.3 m^2/g to 9.1 m^2/g and pore volume from 0.008 cm^3/g to 0.240 cm^3/g.

Similar enhancements are observed in carbide slag when doped with manganese and dolomite, leading to a rise in surface area from 11.1 m^2/g to 14.7 m^2/g. This modification allows the material to achieve a CO_2 capture capacity of 0.52 g CO_2/g sorbent after 10 cycles. However, the utilisation of a single dopant with manganese ions demonstrates an inferior CO_2 capture capacity in comparison.

Moreover, in the case of industrial waste, it has been determined that a pore diameter within the range of 10–100 nm exhibits higher CO_2 capture capacity, reaching approximately 0.63 g CO_2/g sorbent during the first cycle.

4.12.1. Treatment of industrial waste

Industrial waste treatments, such as thermal treatment, recarbonation and hydration are promising approaches to increase the CO_2 capture capacity.

4.12.1.1. Thermal treatment. The pre calcination treatment of pyroligneous acid-modified carbide slag at 400 °C prior calcination process for about 30 min exhibited higher carbonation conversion than acid-modified carbide slag [159]. The pre calcination removes the organic substances that can cause a negative effect during the burning of the organic substances, especially at a temperature of more than 850 °C.

4.12.1.2. Recarbonation. He et al., 2017 [167] studied the effect of re-carbonation in CaL using CS as a calcium precursor. The re-carbonation manages to improve the carbonation conversion slightly even introducing the steam during re-carbonation stages. The re-carbonation causes an extra layer of calcium carbonate to be formed and causes the insufficient unreacted core to exist during carbonation. The thick $CaCO_3$ layer is formed due to the porous structure of CS but collapses after a series of cycles due to sintering and does not increase carbonation conversion considerably. The steam hardly affects the initial kinetics-controlled carbonation stages [168]. Meanwhile, the re-carbonation of carbide slag at the 11th cycles improved the carbonation conversion about 3.1 times at the 13th cycles, higher than 11th cycles, which exhibit a carbonation conversion of 19%. However, the carbonation conversion trend still decreased after several cycles.

4.12.1.3. Hydration. Zhang et al. (2017) [169] introduced the high concentration steam during calcination process of CS by implementing the O_2/H_2O combustion instead high concentration of CO_2. The carbonation conversions of CS at 95% H_2O/5%CO_2 are slightly higher than using 100% CO_2 at 950 °C due to the formation of small grain sizes and porous structure. Steam reduces the calcination temperature, thereby reducing the energy requirement in the calciner to capture per mole CO_2. Moreover, the presence of 5% steam during calcination initiate low initial carbonation conversion than other conditions (calcination: 5 vol% steam/95 vol% air) but demonstrate high stability after 7th cycles when using waste marble powder as CaO sorbent [103].

4.13. Summary of treated industrial waste

Pre-calcination at a temperature of 400 °C has proven effective in increasing CO_2 capture capacity by preventing the combustion of organic substances. This result is attributed to the remarkable increase in surface area, reaching around 14.5 m^2/g. Additionally, recarbonation has been shown to reactivate the sorbent by modifying the pore structure, resulting in a further increase in CO_2 capture capacity.

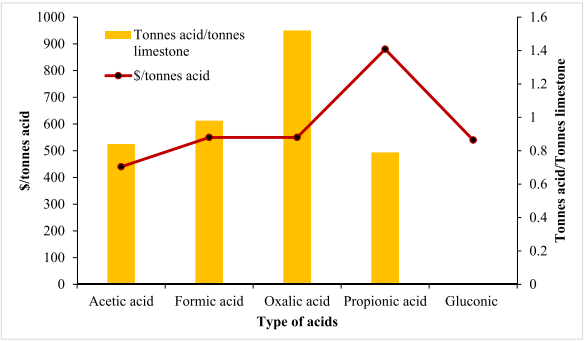

Fig. 8. Cost of the organic acids per tonnes [64] and the acid consumption per tonnes limestone [107].

Furthermore, calcination under high concentrations of steam has demonstrated the formation of small CaO grain sizes and generated a more porous structure, contributing to an additional increase in CO_2 capture capacity. This result highlights the effectiveness of thermal treatment, recarbonation, and hydration as strategies to enhance the overall CO_2 capture capacity of industrial waste.

In summary, the combined treatment of industrial waste through thermal treatment, recarbonation, and hydration proves to be a promising approach for improving CO_2 capture capacity, showcasing the importance of tailored processes to optimise sorbent performance in carbon capture applications.

5. Issues and recommendations

The market penetration of CaL remains challenging due to the great challenges encountered throughout its technological development. This technology is expected to become stable and technologically mature such that it can reduce CO_2 emissions, hence decreasing greenhouse gas emissions. In this section, the issues and challenges of CaO sorbent are extensively discussed, together with the recommendations to overcome the challenges.

5.1. Cost effectiveness of CaO sorbent

One of the major challenges in CaL is to reduce the cost of CaO sorbents. Initially, limestone was widely used as a CaO sorbent due to the low cost, i.e. approximately $0.11/kg in 2023 [64]. However, the sorption capacity has degraded over the few cycles. Thus, alternative CaO sorbents are introduced (e.g. dolomite, biogenesis calcium waste, mangano calcite and industrial waste). The cost of dolomite is $0.10/kg, where no cost for the biogenesis calcium waste and industrial waste. However, several pre-treatments must be developed for biogenesis calcium waste, which can add to the production cost of CaO sorbents. Nevertheless, industrial waste, such as carbide slag, can be used as good alternatives because it exhibits highest sorption capacity amongst other industrial waste. Even though these alternatives demonstrate better carbonation conversion than limestone, the trend of degradation still presents after several cycles. Thus, surface modification of the sorbent such as acid, and doping can improve the carbonation conversion and produce high stability of CaO sorbents. However, the usage of acids increases the cost of the sorbent. Fig. 8 shows the cost of organic acids and the consumption of acid for 1 tonnes of limestone.

Even though the cost of acetic acid is lower than other organic acids, the consumption of 0.84 tonnes acid/tonnes limestone is expected to increase the limestone production cost. Based on the cost estimation of $110/tonnes of limestone and $400/tonnes of acetic acid, the calculation of the operating cost for 1 tonnes of modified limestone is estimated to be approximately $446/tonnes. The operating cost becomes higher when compared with the study by Haran et al. (2021) [170] using limestone at ~$6.73/tonnes. It is still below the expectations which the low-cost sorbent is not achievable. Thus, the usage of waste acid is expected to reduce the CaO cost. PA is a byproduct from plant biomass pyrolysis [171] and can increase the carbonation conversion four times higher than unmodified limestone at severe calcination temperature (960 °C) [112]. Moreover, waste PrA from the pharmaceutical factories, AA produced from anaerobic fermentation and residues, such as sewage sludge can be recycled to obtain the efficient and cheap CaO sorbent [172]. Moreover, the sources of LA, AA, PrA, and CA can be obtained from the waste of cheese manufacture [173].

In addition, the alternatives dopant can be obtained from industrial waste. For example, the usage of waste by-product from magnesium alloy ingot production [174] or solid waste of ductile iron industry that contains of 88% MgO [175] can be used for MgO doping. Meanwhile, saline slag waste [176] and dross [177] can replace Al_2O_3 doping, and the waste of production of dental prostheses from CAD/CAM process can replace the doped zirconium oxide [178]. The usage of these alternatives of CaO precursors, acids and dopants can be used during synthesisation to achieve a low-cost CaO sorbent.

5.2. CO_2 capture capacity of CaO sorbent: mechanical properties

In addition to the discussion above, CO_2 capture capacity was affected by the several mechanical properties such as surface area,

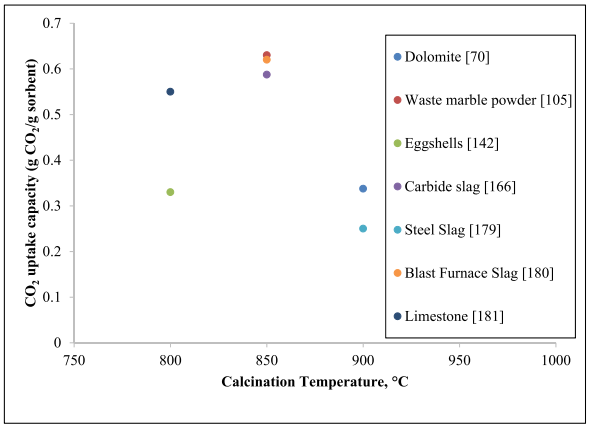

Fig. 9. CO_2 capture capacity of natural precursors and industrial waste.

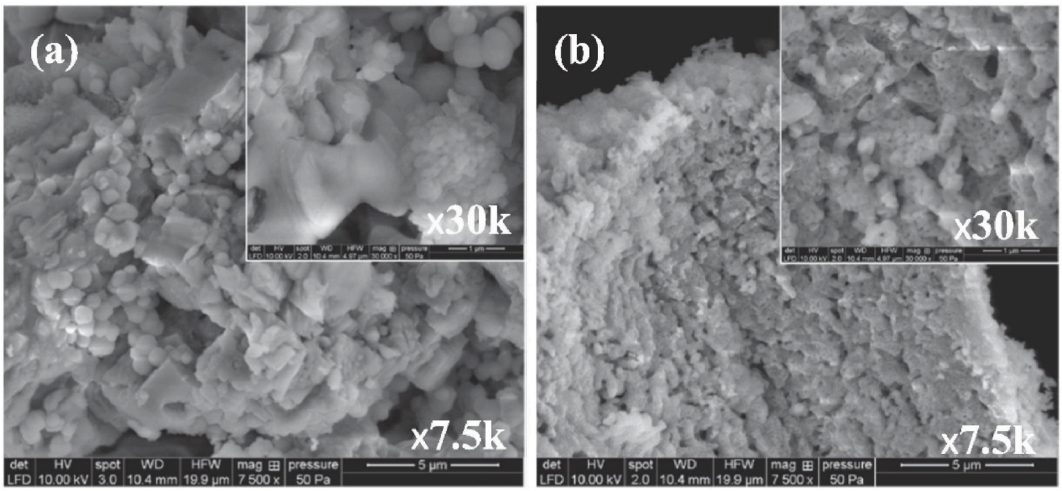

Fig. 10. SEM images of synthesised sorbents at fuel to metal oxide ratio; (a) S20-1x (b) S20-6x. Reproduced from Ref [183].

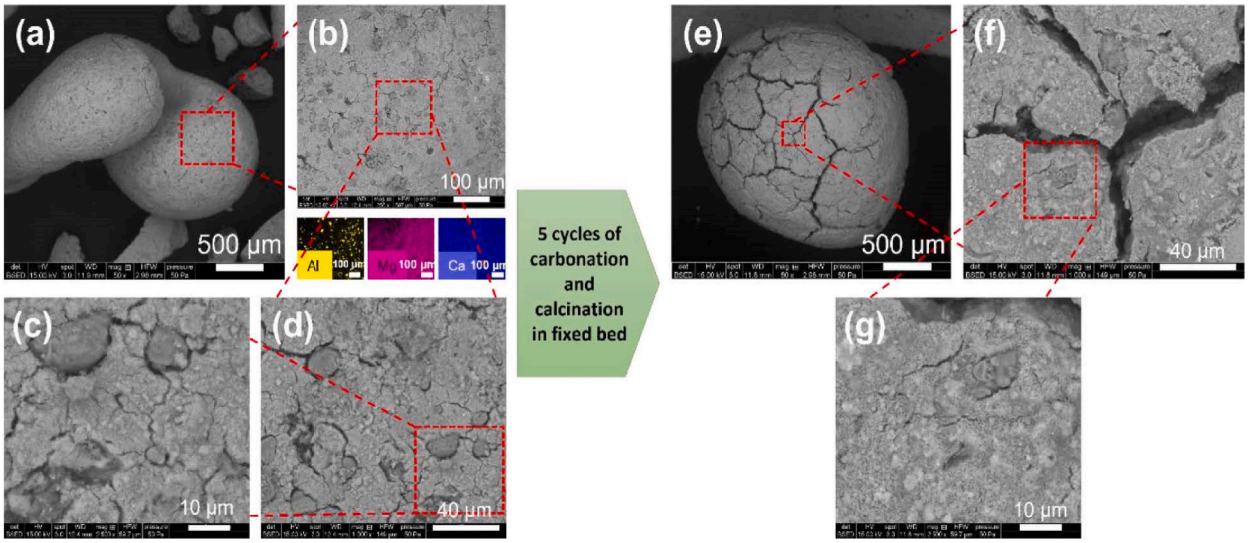

Fig. 11. SEM images of CaO–MgO sorbent (a–d) pre- and (e–g) post-cycling. Ref [184].

Table 7
Improvement of CO_2 capture capacity.

Materials	Methods	Process condition		Cycles	Surface area (m^2/g)		Pore volume (cm^3/g)		Sorption Performance		Ref
		Carbonation	Calcination		Initial	Final	Initial	Final	Initial	Final	
Carbide Slag, Calcium aluminate, $CaAl_2O_4$, rice husk	Extrusion-spheronization	At 650 °C, for 30 min, under 15 vol% CO_2/85 vol % N_2	At 900 °C, for 5 min, under 100 vol% N_2	23	–	–	–	–	0.422 g CO_2/g sorbent	0.15 g CO_2/g sorbent	[194]
Cadomin limestone, Magnesium nitrate hexahydrate, $Mg(NO_3)_2 \cdot 6\ H_2O$, boehmite, γ-AlO(OH)	Solution Combustion Synthesis	At 675 °C, for 20 min, under 20 vol% CO_2/80 vol % N_2	At 850 °C, for 5 min, under 100 vol% N_2	5	28.9	29.3	0.078	0.139	0.48 g CO_2/g sorbent	0.45 g CO_2/g sorbent	[184]
Limestone	–	At 850 °C, for 5 min, under 95 vol% CO_2/5 vol% air	At 950 °C, for 5 min, under 95 vol% CO_2/5 vol % air	20	–	–	–	–	0.68 g CO_2/g sorbent	0.20 g CO_2/g sorbent	[193]
Calcium nitrate, $Ca(NO_3)_2.4H_2O$ Magnesium nitrate, $Mg(NO_3)_2$	Hydrothermal treatment	At 650 °C, for 20 min, under 20 vol% CO_2/80 vol % N_2	At 900 °C, for 10 min, under 100 vol% CO_2	10		7.0		0.084	0.60 g CO_2/g sorbent	0.65 g CO_2/g sorbent	[185]
Ca precursors: Calcium acetylacetonates, $C_{10}H_{14}CaO_4$	Electrospun (2:10)	At 620 °C, for 30 min, under 15 vol% CO_2/85 vol % N_2	At 800 °C, for 20 min, under 100 vol% N_2	50	31.0	12.0	–	–	16.4 mmol/g	6.6 mmol/g	[186]

Table 8
Improvement of stability for CaO sorbent.

Materials	Methods	Process condition		Cycles	Surface area (m^2/g)		Pore volume (cm^3/g)		Sorption Performance		Ref
		Carbonation	Calcination		Initial	Final	Initial	Final	Initial	Final	
Calcium Nitrate, $Ca(NO_3)_2 \cdot xH_2O$, Magnesium Nitrate, $Mg(NO_3)_2 \cdot xH_2O$	Self-sustain combustion	–	–	100	–	–	–	–	61.6% Conversion	52.1% Conversion	[193]
Calcium acetylacetonates, $C_{10}H_{14}CaO_4$, Zirconium acetylacetonates, $C_{20}H_{28}O_8Zr$	Electrospun (2:10)	At 620 °C, for 30 min, under 15 vol% CO_2/85 vol% N_2	At 800 °C, for 20 min, under 100 vol% N_2	50	79.0	54.0	–	–	12.3 mmol/g	10.2 mmol/g	[186]
Calcium nitrate tetrahydrate, $Ca(NO_3)_2.4H_2O$ TEOS, $SiC_8H_{20}O_4$ CTAB, $[(C_{16}H_{33})N(CH_3)_3]Br$, Octadecyl trimethylsilane, $C_{21}H_{46}Si$	Template free	At 650 °C, for 30 min, under 15 vol% CO_2/85 vol% N_2	At 850 °C, for 5 min, under 50 vol% CO_2/50 vol% N_2	10	58.2	25.4	0.280	0.100	0.688 g CO_2/g sorbent	0.627 g CO_2/g sorbent	[199]
Calcium nitrate tetrahydrate, $Ca(NO_3)_2.4H_2O$, Zirconyl nitrate hydrate, $ZrO(NO_3)_2.H_2O$, MWCNT	Facile one pot	At 650 °C, for 10 min, under 15 vol% CO_2/85 vol% N_2	At 650 °C, for 10 min, under 100 vol% CO_2	15	5.0		0.061		0.16 g CO_2/g sorbent	0.104 g CO_2/g sorbent	[188]
Calcium carbonate, $CaCO_3$, Titanium diboride, TiB_2 based nanosheets (f-TBNS)	Dispersion of nanosheet	At 700 °C, for 60 min, under 20 vol% CO_2/80 vol% Ar	At 850 °C, for 10 min, under 100 vol% N_2	8	5.4		0.018		7.75 mmol/g	4.75 mmol/g	[189]
Steel slag, Sodium carbonate, Na_2CO_3		At 700 °C, for 30 min, under 95 vol% CO_2/5 vol% air	At 700 °C, for 30 min, under 95 vol% CO_2/5 vol% air	30	–	–	–	–	14.54 mmol/g	4 mmol/g	[190]
Calcium nitrate tetrahydrate, $Ca(NO_3)_2{\cdot}4H_2O$, Zirconium nitrate pentahydrate, $Zr(NO_3)_4{\cdot}5H_2O$	Sol gel, Graphite Moulding	At 650 °C, for 20 min, under 15 vol% CO_2/85 vol% N_2	At 850 °C, for 10 min, under 15 vol% CO_2/85 vol% N_2	23	–	–	–	–	0.43 g CO_2/g sorbent	0.413 g CO_2/g sorbent	[195]

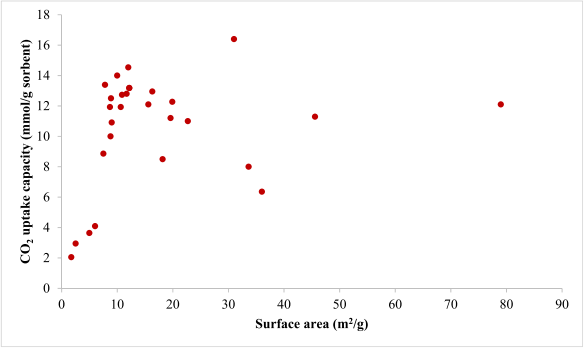

Fig. 12. CO_2 capture capacity of various CaO sorbent at different surface area that is tabulated from Table 9.

pore volume, particle size, and pore diameter.

5.2.1. *Comparison of various CaO sorbent*

Fig. 9 shows that the initial CO_2 capture capacity of natural and waste CaO sorbent are behaves differently. The steel slag (SS) [179] shows the worst CO_2 capture capacity during first cycle compared with dolomite [70] at 900 °C. Meanwhile, WMP [105] shows the highest initial CO_2 capture capacity at 850 °C followed by BFS [180] and CS [166]. Then, the CO_2 capacity of limestone [181] is highest at 800 °C than eggshells [142] during the first cycle.

Therefore, the CaO sorbent precursors and calcination temperature plays an important role in CO_2 capture capacity. Nevertheless, the low cost of limestone and its lack of pre-treatment requirements make it advantageous for industrial applications.

5.2.2. *Morphology of CaO sorbent*

Rodaev et al. (2023) [182] used the electrospun method to produce the nanofiber Ca precursors at low cost and the initial CO_2 capture capacity was found at the highest, 16.4 mmol/g, which is close to the stoichiometric capacity of CaO at 17.9 mmol/g. The CaO nanofibers can absorb more CO_2 than natural CaO sorbent and industrial waste. However, degradation becomes a major issue, especially after 10 cycles. Hashemi et al. (2020) [183] proposed controlling the fuel-to-metal ratio during synthesisation of CaO with zirconium oxide using solution combustion. A higher amount of fuel to metal ratio of 1–6 can improve the initial CO_2 capture capacity due to the fluffy structure and increase in porosity, as shown in Fig. 10(a) and (b). The fluffy structure is less dense and increases the distance between the CaO crystalline grains, decreasing particle sintering.

Hashemi et al. (2022) [184] improved the Cadomin limestone with MgO and boehmite as a binder in pelletisation form. Fig. 11(a) and (b), 11(c), and 11(d) indicates the SEM images of as-it-is CaO–MgO. The study found that the initial CO_2 capture capacity increased in comparison with pure Cadomin limestone. The surface area and pore volume of Cadomin limestone-reinforced MgO was found to be increased after 5 cycles due to the self-reactivation effect that can be seen in Fig. 11(e), (f), and 11(g). Additional cracks appear on CaO sorbents after five cycles, explaining the pore volume increase. However, finer cracks were found at pre-cycling than post cycling due to the sintering effect.

Naeem et al. (2018) [185] investigated the effect of multishelled morphology using hydrothermal treatment. From the study, the formation of highly porous multishelled morphology composed of small nanoparticles increases the CO_2 capture capacity over the cycles.

Rodaev et al., 2023 [186] found that the hollow CaO/Ca_2SiO_4 nanoparticles with diameter of 80–100 nm, and length of 200–600 nm at a Ca/Si molar ratio of 90:10 demonstrates the best CO_2 capture capacity and stability [187]. Furthermore, adding multi-walled carbon nanotubes (MWCNT) at 10% for Ca/Zr demonstrates the highest CO_2 capture capacity and most stable attributes to high surface area amongst other compositions of MWCNT [188]. The fluffy-like morphology reveals the formation of more porous structures and more presence of calcium zirconate amongst the CaO particles. Functionalised TiB_2–based derived nanosheets (f-TBNS) can enhance the capturing capacity due to small size, high surface area, porosity and pore-volume [189]. Moreover, synthesised steel slag demonstrates good anti-sintering properties and is maintained at 11 mmol/g after 30 cycles with the unspecific shapes of sorbent [190]. While nanofiber, nanosheet, nanotubes, and fluffy structures do contribute to the CO_2 capture capacity of CaO sorbent, there is no morphological hindrance to complete carbonation when sufficient time is allowed [191,192].

5.2.3. *Effect of particle size*

Duràn-Martin et al. (2020) [193] studied the effect of particle size on increasing the CO_2 capture capacity. The smaller particle size increases the CO_2 capture capacity and maintains the sorbent stability even after the 20 cycles. However, the fine particles below 50 μm are cohesive and difficult to be fluidised in industrial applications. Therefore, the particle size must be more than 50 μm to be used in the industry, especially to maintain cyclone efficiency during CaL operation in a fluidised bed reactor. The summary of the improvement of CO_2 capture capacity is included in Table 7.

Table 9
CO_2 capture capacity at different surface area and pore volume.

Type of precursors	Methods	Type of samples	Operating Conditions		Cycles	Specific surface area (m^2/g)		Pore volume (cm^3/g)		CO_2 Adsorption		Ref
			Carbonation	Calcination		Initial	Final	Initial	Final	Initial	Final	
Limestone	As-it-is (55.27%), Pore width (33.75 nm)-170um	–	650 °C for 30 min, 15% CO_2, 75% N_2	850 °C for 10 min, 100% N_2	25	12.2	–	0.103	–	13.18 mmol/g sorbent	4.55 mmol/g sorbent	[46]
	–	Ca-5%Bah (19.84 nm)				16.3	–	0.081	–	12.95 mmol/g sorbent	7.95 mmol/g sorbent	
	–	Ca-10%Bah (21.17 nm)				19.9	–	0.105	–	12.27 mmol/g sorbent	7.50 mmol/g sorbent	
	–	Ca-40%Bah (15.6 nm)				36.0	–	0.141	–	6.36 mmol/g sorbent	4.77 mmol/g sorbent	
Carbide Slag	Template synthesis	HT5 (Al_2O_3)	700 °C for 20 min 15% CO_2, 75% N_2	850 °C, 100% N_2	100	12.0	–	0.053	–	14.54 mmol/g sorbent	7.50 mmol/g sorbent	[166]
	As it is	Carbide Slag				10.0	–	0.048	–	14.00 mmol/g sorbent	4.54 mmol/g sorbent	
Calcium and Zirconium acetylacetonates	Electrospun	Pure nanofibrous CaO	620 °C for 30 min, 15% CO_2, 85% N_2	800 °C for 20 min, 100% N_2	50	31.0	12.0	–	–	16.40 mmol/g sorbent	6.60 mmol/g sorbent	[186]
		Zr/Ca molar ratio of 1:10				–	–	–	–	14.20 mmol/g sorbent	8.20 mmol/g sorbent	
		Zr/Ca molar ratio of 2:10				79.0	54.0	–	–	12.10 mmol/g sorbent	9.70 mmol/g sorbent	
		Zr/Ca molar ratio of 3:10				–	–	–	–	10.50 mmol/g sorbent	8.80 mmol/g sorbent	
Pure grade calcium nitrate tetrahydrate, zirconium oxynitrate hexahydrate, and urea	Solution combustion	20% ZrO, 6 fuel to metal oxide ratio	675 °C for 20 min, 20% CO_2, 80% N_2	850 °C for 10 min, 100% N_2	20	19.6	–	0.070	–	11.20 mmol/g sorbent	10.30 mmol/g sorbent	[183]
		20% ZrO, 8 fuel to metal oxide ratio				22.7	–	0.072	–	11.00 mmol/g sorbent	10.30 mmol/g sorbent	
		10% ZrO, 6 fuel to metal oxide ratio				15.6	–	0.057	–	12.10 mmol/g sorbent	9.60 mmol/g sorbent	
Calcium nitrate tetrahydrate from Merck, and zirconyl nitrate	Thermochemical	CaZr	650 °C for 10 min, 15% CO_2, 75% N_2	650 °C for 10 min, 100% CO_2	15	1.8	–	0.025	–	2.05 mmol/g sorbent	0.68 mmol/g sorbent	[188]
		CaZr-CNT2.5				2.5	–	0.0260	–	2.95 mmol/g sorbent	0.91 mmol/g sorbent	

(*continued on next page*)

Table 9 (*continued*)

Type of precursors	Methods	Type of samples	Operating Conditions		Cycles	Specific surface area (m^2/g)		Pore volume (cm^3/g)		CO_2 Adsorption		Ref
			Carbonation	Calcination		Initial	Final	Initial	Final	Initial	Final	
		CaZr-CNT5				6.0	–	0.056	–	4.09 mmol/g sorbent	1.82 mmol/g sorbent	
		CaZr-CNT10				5.0	–	0.0613	–	3.64 mmol/g sorbent	2.27 mmol/g sorbent	
Steel slag		Ca–S	–	–	10	11.7	–	0.087	–	12.80 mmol/g sorbent	11.52 mmol/g sorbent	[190]
Ca-precurosr, Zr-precursors	Sol-gel	Ca95/Zr5	650 °C for 20 min, 15% CO_2, 75% N_2	850 °C for 10 min,	–	7.8	–	0.011	–	13.39 mmol/g sorbent	10.68 mmol/g sorbent	[195]
		Ca90/Zr10				8.9	–	0.011	–	12.50 mmol/g sorbent	10.23 mmol/g sorbent	
		Ca85/Zr15				8.7	–	0.013	–	11.93 mmol/g sorbent	10.00 mmol/g sorbent	
		Ca80/Zr20				10.6	–	0.015	–	9.7.0 mmol/g sorbent	9.60 mmol/g sorbent	
Crab shell, CTAB, PEG	Hydrothermal	Temp = 550 °C	600 °C, 100% CO_2	800 °C, 100% Ar	4	33.6	–	–	–	8.00 mmol/g sorbent	3.69 mmol/g sorbent	[200]
Nano $CaCO_3$	Template	Ca	650 °C for 20 min, 15% CO_2, 75% N_2	850 °C for 10 min, 100% N_2	15	7.5	–	0.007	–	8.86 mmol/g sorbent	3.64 mmol/g sorbent	[201]
		Ca-Starch				9.0	–	0.036	–	10.91 mmol/g sorbent	5.68 mmol/g sorbent	
		Ca-CNT				12.2	–	0.014	–	13.18 mmol/g sorbent	8.64 mmol/g sorbent	
		Ca-Carbon Nanofibres				10.9	–	0.013	–	12.73 mmol/g sorbent	6.82 mmol/g sorbent	
		Cotton Fibre				8.8	–	0.033	–	10.00 mmol/g sorbent	5.23 mmol/g sorbent	
Dolomite	As-it-is	–	650 °C for 20 min, 15% CO_2, 75% N_2	850 °C for 10 min, 100% N_2	10	45.6	–	0.122	–	11.29 mmol/g sorbent	9.80 mmol/g sorbent	Exp
Limestone		–				18.2	–	0.057	–	8.50 mmol/g sorbent	5.39 mmol/g sorbent	

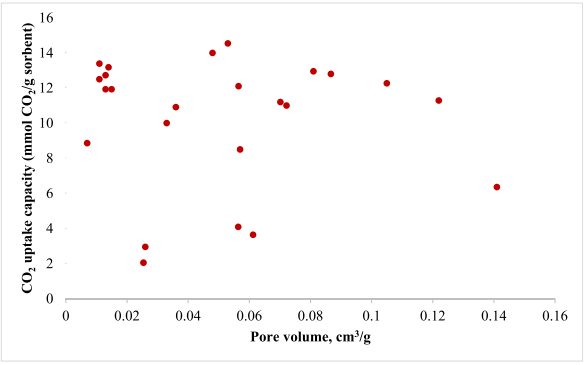

Fig. 13. CO_2 capture capacity of various CaO sorbent at different pore volume that is tabulated from Table 9.

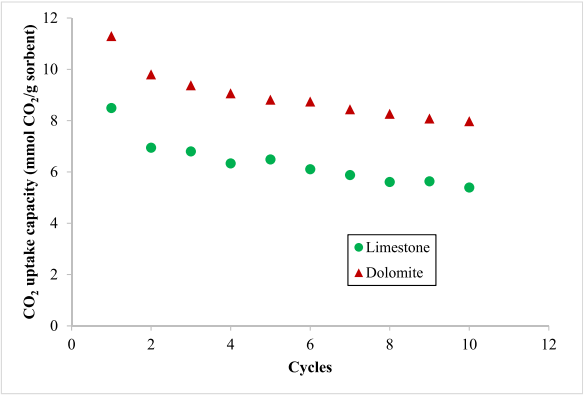

Fig. 14. CO_2 capture capacity of limestone and dolomite at carbonation 650 °C with 15% CO_2, 85% N_2 for 20 min, and calcination at 850 °C with 100% N_2 for 10 min.

5.2.4. *Effect of preparation methods*

In addition to CaO precursors, preparation methods for CaO sorbents also affected the CO_2 capture capacity. Preparation methods, such as sol–gel demonstrates the highest CO_2 capture capacity and most stable (0.53 g CO_2/g sorbent [first cycle] – 0.439 g CO_2/g sorbent [17 cycles]) compared with hydration–mixing and wet mixing due to uniform distribution of inert $CaZrO_3$ spacer [195]. Wang et al. (2018) [196] investigated the effect of preparation methods on the performance of the Al-stabilised CaO sorbents for capturing CO_2. The CO_2 capture capacity of CaO sorbents when incorporated with Al_2O_3 using sol-gel methods is higher than co-precipitation and wet mixing due to increased surface area and small crystallite size, thus increasing the CO_2 capture capacity of synthetic sorbent. Moreover, the main contribution of the high CO_2 capture capacity when using sol–gel method is due to the CaO precursors and the supporting material that are homogenously dispersed to produce a stable structure. Furthermore, Zr– and Ce–doped sorbents using sol–gel increase the CO_2 capture capacity and can maintain the stability after several cycles due to the formation of $CaZrO_3$ that has high Tammann temperature (1218 °C). In addition, CeO_2 provides rich oxygen vacancies and could facilitate the migration of O^{2-} into the CaO structure. Combinations, especially sol–gel combustion, can produce approximately 0.66 g CO_2/g sorbent [197]. However, the stability of CaO sorbent when combining sol–gel with graphite–moulding is higher than the sol–gel method [198].

Furthermore, sea salt–doped limestone, achieved through a simultaneous hydration-impregnation method, demonstrates a notable CO_2 capture capacity of 0.31 g CO_2/g sorbent after 40 cycles [44]. The simultaneous hydration-impregnation method enhanced CO_2 capture capacity at any sea-water concentration. Moreover, adding rice husk to the carbide slag binded calcium aluminate using the extrusion-spheronisation method can increase the initial CO_2 capture capacity. Even though marginal improvement was exhibited, the preparation method is simple and uses inexpensive material [194]. Thus, the preparation methods are important in enhancing the CO_2 capture capacity. The summary of the improvement for CaO sorbent is included in Table 8.

5.2.5. *Effect of surface area and pore volume*

Researchers reported that CO_2 capture capacity was affected by properties of CaO sorbent, such as surface area, pore volume, and particle size. However, based on data from previous research, BET surface area plays a minimal role in determining the initial CO_2 capture capacity of CaO sorbent. Fig. 12 shows that the CaO sorbent that acquires a BET surface area of 7–20 m^2/g is sufficient to exhibit 12–15 mmol/g sorbent at initial CO_2 capture capacity. The 17.8 mmol/g sorbent of CO_2 capture capacity is the highest CO_2 capture capacity based on stoichiometric capacity. Thus, a higher BET surface area than 20 m^2/g does not warrant a higher initial CO_2 capture capacity of CaO sorbent.

Furthermore, the pore volume does not affect the initial CO_2 capture capacity, as shown in Fig. 13. An experiment was conducted to prove this statement, as shown in Fig. 14 and Table 9. The surface area of limestone and dolomite is 18.2 m^2/g and 45.6 m^2/g, respectively. Limestone demonstrates the CO_2 capture capacity from 8.49 mmol/g sorbent to 4.39 mmol/g sorbent after 10 cycles. Meanwhile, dolomite exhibits a CO_2 capture capacity from 11.29 mmol/g sorbent until 7.98 mmol/g sorbent after 10 cycles. Even though a high surface area benefits the CO_2 capture capacity, it does not considerably affect the CO_2 capture capacity. Previous studies found that active CaO is needed to have high CO_2 capture capacity and when reinforced with other materials can maintain the stability of CO_2 uptake capacity by improving the anti-sintering properties. The summary of the surface area and pore volume for CaO sorbents is included in Table 9.

6. Conclusions

CaL stands out as a promising technology for CO_2 capture. However, the issue of sorbent degradation poses a considerable challenge because the loss of sorbent is linked to an increase in sorbent replacement. This review extensively examines the CO_2 capture capacity and carbonation conversion of various CaO precursors, classified into natural and industrial waste CaO sorbents.

Limestone and industrial waste show high CO_2 capture capacity, making them advantageous due to their availability and cost-effectiveness. Modification using organic acids enhances the CO_2 capture capacity of limestone, biogenesis calcium waste, and industrial waste. However, sorbent degradation follows a similar trend to untreated CaO sorbent, indicating that acid modification does not maintain stability over several cycles. The use of waste acid in acid modifications can help reduce operational costs.

Furthermore, the introduction of dopant materials enhances the stability of both natural and industrial waste CaO sorbents, given that the dopant exhibits a high Tammann temperature, consequently improving anti-sintering properties. Enhanced sorbent stability ensures that the CO_2 capture capacity can persist close to the theoretical value of 0.786 g CO_2/g sorbent even after 20 cycles. This reduction in the need for sorbent replenishment contributes to a decrease in operational costs. Dopant waste can be used to reduce the cost during synthesisation. Additionally, pre-treatment, hydration, thermal treatment, and reactivation contribute to improving the CO_2 capture capacity and stability of these sorbents.

In summary, the morphology of a CaO sorbent has minimal impact on CO_2 capture capacity, with modifications yielding irrelevant effects on CO_2 adsorption. However, high fractal dimensions are essential for achieving high CO_2 capture capacity because they facilitate increased adsorption which can be controlled during the synthesising. Nanostructures enhance CO_2 capture capacity, but for practical industrial applications, the particle size should exceed 50 μm. An optimal surface area of 7–20 m^2/g is sufficient for achieving high CO_2 capture capacity, and pore volume does not significantly affect CO_2 capture capacity. The presence of mesopores (2 nm–100 nm) in the pore size distribution is crucial for enhancing the CO_2 capture capacity of modified sorbents.

Hence, this review offers valuable perspectives on the prospective advancements in CaL technology, with a specific emphasis on its application in carbon capture. The focus is primarily directed towards the enhancements made to CaO sorbents and the properties influencing CO_2 capture capacity.

CRediT authorship contribution statement

Nurfanizan Afandi: Writing – original draft, Funding acquisition. **Meenaloshini Satgunam:** Writing – review & editing. **Savisha Mahalingam:** Writing – review & editing. **Abreeza Manap:** Writing – review & editing. **Farrukh Nagi:** Supervision, Project administration, Conceptualization. **Wen Liu:** Writing – review & editing. **Rafie Bin Johan:** Supervision, Funding acquisition. **Ahmet Turan:** Supervision. **Adrian Wei-Yee Tan:** Supervision. **Salmi Yunus:** Writing – review & editing.

Declaration of competing interest

The authors declare the following financial interests/personal relationships which may be considered as potential competing interests: Nurfanizan Binti Mohd Afandi reports financial support was provided by National Energy University.

Acknowledgment

This work was supported by Ministry of Higher Education, Malaysia through the Fundamental of research Grant (FRGS), under the project code of 20231008FRGS, Higher Institution Centre of Excellence, under the project code of 2022002HICOE and Tenaga Nasional Berhad (TNB), and UNITEN through the BOLD Research Grant under the project code of J510050002/2022031.

List of abbreviations and symbols

CaL	Calcium looping cycle
CO_2	Carbon dioxide
AA	Acetic acid
BAh	Bayer aluminium hydroxide
BET	Brunauer-Emmett-Teller
BFS	Blast furnace slag
BMCR	Ball milling–assisted carbonation conversion reactivation

CA	Citric acid
$CaCO_3$	Calcium carbonate
CaO	Calcium oxide
CIMPOR	Cimentos de Portugal, E.P.
Cl	Chlorine
CS	Carbide slag
FA	Formic acid
Fe	Ferum
f-TBNS	Functionalised TiB_2–based derived nanosheets
GA	Gluconic acid
K	Potassium
LA	Lactic acid
LM	Lime mud
MA	Malic acid
Mn	Manganese
MWCNT	Multi-walled carbon nanotubes
N_2	Nitrogen
NA	Nitric acid
Na	Sodium
OA	Oxalic acid
P	Phosporus
PA	Pyroligneous acid
PrA	Propionic acid
PVC	Polyvinyl chloride
S	Sulphur
SEM	Scanning electron microscopy
SO_2	Sulphur dioxide
Sr	Strontium
TA	Tartaric acid
WMP	Waste marble powder
X_D	Molar conversion under the diffusion-controlled stage
X_K	Molar conversion under the fast reaction regime
$	US Dollar
°C	Celcius
m_0	Initial mass at each cycle
m_f	Mass of the sorbent at the end of carbonation at each cycle
x	mass fraction of the active CaO in the cycle

Data Availability Statement

The data will be made available upon request.

References

[1] IEA, CO_2 emissions in 2022, Glob. Energy. 62 (2022) 20–21. https://www.iea.org/news/global-co2-emissions-rebounded-to-their-highest-level-in-history-in-2021.

[2] 242bb71eba13a40a8addb4fdd52ca8b185525340 @ themalaysianreserve.com, 2021. https://themalaysianreserve.com/2021/08/04/govt-expands-unconditional-national-determined-contributions-to-45/.

[3] W.H. Tsai, Carbon emission reduction-carbon tax, carbon trading, and carbon offset, Energies 13 (2020) 6128, https://doi.org/10.3390/en13226128.

[4] A. Ghazouani, W. Xia, M. Ben Jebli, U. Shahzad, Exploring the role of carbon taxation policies on CO_2 emissions: contextual evidence from tax implementation and non-implementation european countries, Sustain. Times 12 (2020) 8680, https://doi.org/10.3390/su12208680.

[5] R. Li, M. Su, The role of natural gas and renewable energy in curbing carbon emission: case study of the United States, Sustain. Times 9 (2017) 600, https://doi.org/10.3390/su9040600.

[6] S.N.A. Latif, M.S. Chiong, S. Rajoo, A. Takada, Y.Y. Chun, K. Tahara, Y. Ikegami, The trend and status of energy resources and greenhouse gas emissions in the Malaysia power generation mix, Energies 14 (2021) 2200, https://doi.org/10.3390/en14082200.

[7] L. Xue, M. Haseeb, H. Mahmood, T.T.Y. Alkhateeb, M. Murshed, Renewable energy use and ecological footprints mitigation: evidence from selected south asian economies, Sustain. Times 13 (2021) 1–20, https://doi.org/10.3390/su13041613.

[8] R.J. Campbell, Increasing the efficiency of existing coal-fired power plants, in: Coal-Fired Power Plants Effic. Improv. Options, Nova Science Publishers, Inc, 2015, pp. 77–111.

[9] A. Raza, R. Gholami, R. Rezaee, V. Rasouli, M. Rabiei, Significant aspects of carbon capture and storage – a review, Petroleum 5 (2019) 335–340, https://doi.org/10.1016/j.petlm.2018.12.007.

[10] A.I. Osman, M. Hefny, M.I.A. Abdel Maksoud, A.M. Elgarahy, D.W. Rooney, Recent Advances in Carbon Capture Storage and Utilisation Technologies: a Review, Springer International Publishing, 2021, https://doi.org/10.1007/s10311-020-01133-3.

[11] J. Singh, D.W. Dhar, Overview of carbon capture technology: microalgal biorefinery concept and state-of-the-art, Front. Mar. Sci. 6 (2019) 1–9, https://doi.org/10.3389/fmars.2019.00029.
[12] Coal Explained Coal Prices and Outlook, U.S. Energy Inf. Adm., 2022. https://www.eia.gov/energyexplained/coal/prices-and-outlook.php.
[13] Y. Wang, L. Zhao, A. Otto, M. Robinius, D. Stolten, A review of post-combustion CO_2 capture technologies from coal-fired power plants, Energy Proc. 114 (2017) 650–665, https://doi.org/10.1016/j.egypro.2017.03.1209.
[14] P. Madejski, K. Chmiel, N. Subramanian, T. Kus, Methods and techniques for CO_2 capture : review of potential, Energies 15 (2022) 887.
[15] X. Li, Z. Peng, Y. Pei, T. Ajmal, K.J. Rana, A. Aitouche, R. Mobasheri, Oxy-fuel combustion for carbon capture and storage in internal combustion engines – a review, Int. J. Energy Res. 46 (2022) 505–522, https://doi.org/10.1002/er.7199.
[16] L. Jiang, A. Gonzalez-Diaz, J. Ling-Chin, A.P. Roskilly, A.J. Smallbone, Post-combustion CO_2 capture from a natural gas combined cycle power plant using activated carbon adsorption, Appl. Energy 245 (2019) 1–15, https://doi.org/10.1016/j.apenergy.2019.04.006.
[17] T. Shimizu, T. Hirama, H. Hosoda, K. Kitano, M. Inagaki, K. Tejima, A twin fluid-bed reactor for removal of CO_2 from combustion processes, Chem. Eng. Res. Des. 77 (1999) 62–68, https://doi.org/10.1205/026387699525882.
[18] H. Dieter, A.R. Bidwe, G. Varela-Duelli, A. Charitos, C. Hawthorne, G. Scheffknecht, Development of the Calcium Looping CO_2 Capture Technology from Lab to Pilot Scale at IFK, vol. 127, University of Stuttgart, Fuel, 2014, pp. 23–37, https://doi.org/10.1016/j.fuel.2014.01.063.
[19] A. MacKenzie, D.L. Granatstein, E.J. Anthony, J.C. Abanades, Economics of CO_2 capture using the calcium cycle with a pressurized fluidized bed combustor, Energy Fuel. 21 (2007) 920–926, https://doi.org/10.1021/ef0603378.
[20] R.T. Symonds, D.Y. Lu, A. Macchi, R.W. Hughes, E.J. Anthony, CO_2 capture from syngas via cyclic carbonation/calcination for a naturally occurring limestone: modelling and bench-scale testing, Chem. Eng. Sci. 64 (2009) 3536–3543, https://doi.org/10.1016/j.ces.2009.04.043.
[21] T. Papalas, A.N. Antzaras, A.A. Lemonidou, Evaluation of calcium-based sorbents derived from natural ores and industrial wastes for high-temperature CO_2 capture, Ind. Eng. Chem. Res. 59 (2020) 9926–9938, https://doi.org/10.1021/acs.iecr.9b06834.
[22] Y. Yan, K. Wang, P.T. Clough, E.J. Anthony, Developments in calcium/chemical looping and metal oxide redox cycles for high-temperature thermochemical energy storage: a review, Fuel Process, Technol. 199 (2020) 106280, https://doi.org/10.1016/j.fuproc.2019.106280.
[23] C. Ortiz, J.M. Valverde, R. Chacartegui, L.A. Pérez-Maqueda, P. Gimenez-Gavarrell, Scaling-up the calcium-looping process for CO_2 capture and energy storage, KONA Powder Part. J. 38 (2021) 189–208, https://doi.org/10.14356/kona.2021005.
[24] M.G. Plaza, S. Mart, F. Rubiera, Cement industry : state of the art and expectations, Energies 13 (2020) 5692, https://doi.org/10.3390/en13215692.
[25] F.J. Durán-Olivencia, M.J. Espín, J.M. Valverde, Cross effect between temperature and consolidation on the flow behavior of granular materials in thermal energy storage systems, Powder Technol. 363 (2020) 135–145, https://doi.org/10.1016/j.powtec.2019.11.125.
[26] C.C. Dean, J. Blamey, N.H. Florin, M.J. Al-Jeboori, P.S. Fennell, The calcium looping cycle for CO_2 capture from power generation, cement manufacture and hydrogen production, Chem. Eng. Res. Des. 89 (2011) 836–855, https://doi.org/10.1016/j.cherd.2010.10.013.
[27] J. Sun, W. Wang, Y. Yang, S. Cheng, Y. Guo, C. Zhao, W. Liu, P. Lu, Reactivation mode investigation of spent CaO-based sorbent subjected to CO_2 looping cycles or sulfation, Fuel 266 (2020) 117056, https://doi.org/10.1016/j.fuel.2020.117056.
[28] J. Chen, L. Duan, Z. Sun, Review on the development of sorbents for calcium looping, Energy Fuel. 34 (2020) 7806–7836, https://doi.org/10.1021/acs.energyfuels.0c00682.
[29] M. Strojny, P. Gładysz, D.P. Hanak, W. Nowak, Comparative analysis of CO_2 capture technologies using amine absorption and calcium looping integrated with natural gas combined cycle power plant, Energy 284 (2023), https://doi.org/10.1016/j.energy.2023.128599.
[30] S. Sun, Z. Lv, Y. Qiao, C. Qin, S. Xu, C. Wu, Integrated CO_2 capture and utilization with CaO-alone for high purity syngas production, Carbon Capture, Sci. Technol. 1 (2021) 100001, https://doi.org/10.1016/j.ccst.2021.100001.
[31] J. Cai, F. Yan, M. Luo, S. Wang, Highly stable CO_2 capture performance of binary doped carbide slag synthesized through liquid precipitation method, Fuel 280 (2020) 118575, https://doi.org/10.1016/j.fuel.2020.118575.
[32] H. Liu, S. Wu, Preparation of high sorption durability nano-CaO-ZnO CO_2 adsorbent, Energy Fuel. 33 (2019) 7626–7633, https://doi.org/10.1021/acs.energyfuels.9b01770.
[33] X. Liang, H. Chen, Utilization of biomass to promote calcium-based sorbents for CO_2 capture, Greenh. Gases Sci. Technol. 11 (2021) 837–855, https://doi.org/10.1002/ghg.2083.
[34] M. Erans, V. Manovic, E.J. Anthony, Calcium looping sorbents for CO_2 capture, Appl. Energy 180 (2016) 722–742, https://doi.org/10.1016/j.apenergy.2016.07.074.
[35] J. Blamey, E.J. Anthony, J. Wang, P.S. Fennell, The calcium looping cycle for large-scale CO_2 capture, Prog. Energy Combust. Sci. 36 (2010) 260–279, https://doi.org/10.1016/j.pecs.2009.10.001.
[36] W. Liu, H. An, C. Qin, J. Yin, G. Wang, B. Feng, M. Xu, Performance enhancement of calcium oxide sorbents for cyclic CO_2 capture-a review, Energy Fuel. 26 (2012) 2751–2767, https://doi.org/10.1021/ef300220x.
[37] J.M. Valverde, Ca-based synthetic materials with enhanced CO_2 capture efficiency, J. Mater. Chem. A 1 (2013) 447–468, https://doi.org/10.1039/c2ta00096b.
[38] A. Perejón, L.M. Romeo, Y. Lara, P. Lisbona, A. Martínez, J.M. Valverde, The Calcium-Looping technology for CO_2 capture: on the important roles of energy integration and sorbent behavior, Appl. Energy 162 (2016) 787–807, https://doi.org/10.1016/j.apenergy.2015.10.121.
[39] H. Sun, C. Wu, B. Shen, X. Zhang, Y. Zhang, J. Huang, Progress in the development and application of CaO-based adsorbents for CO_2 capture—a review, Mater. Today Sustain. 1–2 (2018) 1–27, https://doi.org/10.1016/j.mtsust.2018.08.001.
[40] Y. Hu, H. Lu, W. Liu, Y. Yang, H. Li, Incorporation of CaO into inert supports for enhanced CO_2 capture: a review, Chem. Eng. J. 396 (2020) 125253, https://doi.org/10.1016/j.cej.2020.125253.
[41] M.T. Dunstan, F. Donat, A.H. Bork, C.P. Grey, C.R. Müller, CO_2 capture at medium to high temperature using solid oxide-based sorbents: fundamental aspects, mechanistic insights, and recent advances, Chem. Rev. 121 (2021) 12681–12745, https://doi.org/10.1021/acs.chemrev.1c00100.
[42] T. Luo, S. Liu, C. Luo, X. Qi, B. Lu, L. Zhang, Effect of different organic compounds on the preparation of CaO-based CO_2 sorbents derived from wet mixing combustion synthesis, Chin. J. Chem. Eng. 36 (2021) 157–169, https://doi.org/10.1016/j.cjche.2020.09.039.
[43] Y. Xu, C. Lu, C. Luo, G. Wang, X. Yan, G. Gao, B. Lu, F. Wu, L. Zhang, Thermochemical energy storage by calcium looping process that integrates CO_2 power cycle and steam power cycle, Fuel Process. Technol. 242 (2023) 107656, https://doi.org/10.1016/j.fuproc.2023.107656.
[44] Y. Xu, C. Luo, Y. Zheng, H. Ding, L. Zhang, Macropore-Stabilized limestone sorbents prepared by the simultaneous hydration-impregnation method for high-temperature CO_2 capture, Energy Fuel. 30 (2016) 3219–3226, https://doi.org/10.1021/acs.energyfuels.5b02603.
[45] W. Zhao, Y. Li, Y. Yang, F. Wang, Revealing co-promotion mechanism of Mn/$Ca_3Al_2O_6$ on CO_2 adsorption performance of CaO in calcium looping by density functional theory, Sep. Purif. Technol. 329 (2024) 125165, https://doi.org/10.1016/j.seppur.2023.125165.
[46] J. Sun, W. Liu, M. Li, X. Yang, W. Wang, Y. Hu, H. Chen, X. Li, M. Xu, Mechanical modification of naturally occurring limestone for high-temperature CO_2 capture, Energy Fuel. 30 (2016) 6597–6605, https://doi.org/10.1021/acs.energyfuels.6b01131.
[47] Y. Da, J. Zhou, Multi-doping strategy modified calcium-based materials for improving the performance of direct solar-driven calcium looping thermochemical energy storage, Sol. Energy Mater. Sol. Cells 238 (2022) 111613, https://doi.org/10.1016/j.solmat.2022.111613.
[48] X. Kou, C. Li, Y. Zhao, S. Wang, X. Ma, CO_2 sorbents derived from capsule-connected Ca-Al hydrotalcite-like via low-saturated coprecipitation, Fuel Process. Technol. 177 (2018) 210–218, https://doi.org/10.1016/j.fuproc.2018.04.036.
[49] C. Luo, Y. Zheng, Y. Xu, N. Ding, Q. Shen, C. Zheng, Wet mixing combustion synthesis of CaO-based sorbents for high temperature cyclic CO_2 capture, Chem. Eng. J. 267 (2015) 111–116, https://doi.org/10.1016/j.cej.2015.01.005.
[50] F.D.M. Daud, M.M.M. Azir, M.S. Mahmud, N. Sarifuddin, H.H.M. Zaki, Preparation of cao-based pellet using rice husk ash via granulation method for potential CO_2 capture, IIUM Eng. J. 22 (2021) 234–244, https://doi.org/10.31436/IIUMEJ.V22I1.1544.

[51] J. Chen, L. Duan, T. Shi, R. Bian, Y. Lu, F. Donat, E.J. Anthony, A facile one-pot synthesis of CaO/CuO hollow microspheres featuring highly porous shells for enhanced CO_2 capture in a combined Ca-Cu looping process: via a template-free synthesis approach, J. Mater. Chem. A 7 (2019) 21096–21105, https://doi.org/10.1039/c9ta04513a.

[52] M.A. Naeem, A. Armutlulu, Q. Imtiaz, C.R. Müller, CaO-based CO_2 sorbents effectively stabilized by metal oxides, ChemPhysChem 18 (2017) 3280–3285, https://doi.org/10.1002/cphc.201700695.

[53] R. Koirala, G.K. Reddy, P.G. Smirniotis, Single nozzle flame-made highly durable metal doped ca-based sorbents for CO_2 capture at high temperature, Energy Fuel. 26 (2012) 3103–3109, https://doi.org/10.1021/ef3004015.

[54] M. Alonso, B. Arias, J.R. Fernández, O. Bughin, C. Abanades, Measuring attrition properties of calcium looping materials in a 30 kW pilot plant, Powder Technol. 336 (2018) 273–281, https://doi.org/10.1016/j.powtec.2018.06.011.

[55] P.H. Chang, H.P. Hsu, S.C. Wu, C.H. Peng, Synthesis and formation mechanism of limestone-derived porous rod hierarchical Ca-based metal–organic framework for efficient CO_2 capture, Materials 13 (2020) 4297, https://doi.org/10.3390/ma13194297.

[56] C. Wang, X. Zhou, L. Jia, Y. Tan, Sintering of limestone in calcination/carbonation cycles, Ind. Eng. Chem. Res. 53 (2014) 16235–16244, https://doi.org/10.1021/ie502069d.

[57] J. Niu, M. Li, B. Wang, F. Yu, A. Tao, S. Li, Y. Wu, Catalyzed sintering of regenerated CaO induced by partition evolution of calcium carbonate, Chem. Eng. Technol. 44 (2021) 495–502, https://doi.org/10.1002/ceat.202000368.

[58] L.M. Romeo, Y. Lara, P. Lisbona, J.M. Escosa, Optimizing make-up flow in a CO_2 capture system using CaO, Chem. Eng. J. 147 (2009) 252–258, https://doi.org/10.1016/j.cej.2008.07.010.

[59] H. Gupta, L.S. Fan, Carbonation-calcination cycle using high reactivity calcium oxide for carbon dioxide separation from flue gas, Ind. Eng. Chem. Res. 41 (2002) 4035–4042, https://doi.org/10.1021/ie010867l.

[60] S. Medina-Carrasco, J.M. Valverde, The Calcium Looping process for energy storage: insights from in situ XRD analysis, Chem. Eng. J. 429 (2022) 132244, https://doi.org/10.1016/j.cej.2021.132244.

[61] Y. Xu, C. Luo, Y. Zheng, H. Ding, Q. Wang, Q. Shen, X. Li, L. Zhang, Characteristics and performance of CaO-based high temperature CO_2 sorbents derived from a sol-gel process with different supports, RSC Adv. 6 (2016) 79285–79296, https://doi.org/10.1039/c6ra15785h.

[62] M.A. Naeem, A. Armutlulu, A. Kierzkowska, C.R. Müller, Development of high-performance CaO-based CO_2 sorbents stabilized with Al_2O_3 or MgO, Energy Proc. 114 (2017) 158–166, https://doi.org/10.1016/j.egypro.2017.03.1158.

[63] A.A. Scaltsoyiannes, A.A. Lemonidou, On the factors affecting the deactivation of limestone under calcium looping conditions: a new comprehensive model, Chem. Eng. Sci. 243 (2021) 116797, https://doi.org/10.1016/j.ces.2021.116797.

[64] alibaba.com, Search @ Www.Alibaba.Com, (n.d.). http://www.alibaba.com/trade/search?fsb=y&IndexArea=product_en&CatId=&SearchText=magnesite+oxide+price.

[65] Z. Zhao, K. Patchigolla, Y. Wu, J. Oakey, E.J. Anthony, H. Chen, Performance study on Ca-based sorbents for sequential CO_2 and SO_2 capture in a bubbling fluidised bed, Fuel Process. Technol. 221 (2021) 106938, https://doi.org/10.1016/j.fuproc.2021.106938.

[66] R. Han, Y. Wang, S. Xing, C. Pang, Y. Hao, C. Song, Q. Liu, Progress in reducing calcination reaction temperature of Calcium-Looping CO_2 capture technology: a critical review, Chem. Eng. J. 450 (2022) 137952, https://doi.org/10.1016/j.cej.2022.137952.

[67] K. Wang, Z. Yin, P. Zhao, D. Han, X. Hu, G. Zhang, Effect of chemical and physical treatments on the properties of a dolomite used in Ca looping, Energy Fuel. 29 (2015) 4428–4435, https://doi.org/10.1021/acs.energyfuels.5b00853.

[68] Y. Duan, D. Luebke, H. Henry Pennline, Efficient theoretical screening of solid sorbents for CO_2 capture applications, Int. J. Clean Coal Energy 1 (2012) 1–11, https://doi.org/10.4236/ijcce.2012.11001.

[69] A. Hassanzadeh, J. Abbasian, Regenerable MgO-based sorbents for high-temperature CO_2 removal from syngas: 1. Sorbent development, evaluation, and reaction modeling, Fuel 89 (2010) 1287–1297, https://doi.org/10.1016/j.fuel.2009.11.017.

[70] A. De La Calle Martos, J.M. Valverde, P.E. Sanchez-Jimenez, A. Perejón, C. García-Garrido, L.A. Perez-Maqueda, Effect of dolomite decomposition under CO_2 on its multicycle CO_2 capture behaviour under calcium looping conditions, Phys. Chem. Chem. Phys. 18 (2016) 16325–16336, https://doi.org/10.1039/c6cp01149g.

[71] Y. Su, R. Han, J. Gao, S. Wei, F. Sun, G. Zhao, Novel method for regeneration/reactivation of spent dolomite-based sorbents from calcium looping cycles, Chem. Eng. J. 360 (2019) 148–156, https://doi.org/10.1016/j.cej.2018.11.095.

[72] P. Teixeira, A. Fernandes, F. Ribeiro, C.I.C. Pinheiro, Blending wastes of marble powder and dolomite sorbents for calcium-looping CO_2 capture under realistic industrial calcination conditions, Materials 14 (2021) 4379, https://doi.org/10.3390/ma14164379.

[73] S. Castilho, A. Kiennemann, M.F. Costa Pereira, A.P. Soares Dias, Sorbents for CO_2 capture from biogenesis calcium wastes, Chem. Eng. J. 226 (2013) 146–153, https://doi.org/10.1016/j.cej.2013.04.017.

[74] A. Hart, H. Onyeaka, Eggshell and seashells biomaterials sorbent for carbon dioxide capture, in: Carbon Capture, IntechOpen, 2021, https://doi.org/10.5772/intechopen.93870.

[75] S.A. Salaudeen, S.H. Tasnim, M. Heidari, B. Acharya, A. Dutta, Eggshell as a potential CO_2 sorbent in the calcium looping gasification of biomass, Waste Manag. 80 (2018) 274–284, https://doi.org/10.1016/j.wasman.2018.09.027.

[76] M. Ives, R.C. Mundy, P.S. Fennell, J.F. Davidson, J.S. Dennis, A.N. Hayhurst, Comparison of different natural sorbents for removing CO_2 from combustion gases, as studied in a bench-scale fluidized bed, Energy Fuel. 22 (2008) 3852–3857, https://doi.org/10.1021/ef800417v.

[77] Y. Hu, W. Liu, W. Wang, J. Sun, X. Yang, H. Chen, M. Xu, Investigation of novel naturally occurring manganocalcite for CO_2 capture under oxy-fuel calcination, Chem. Eng. J. 296 (2016) 412–419, https://doi.org/10.1016/j.cej.2016.03.134.

[78] J.M. Valverde, P.E. Sanchez-Jimenez, L.A. Perez-Maqueda, Ca-looping for postcombustion CO_2 capture: a comparative analysis on the performances of dolomite and limestone, Appl. Energy 138 (2015) 202–215, https://doi.org/10.1016/j.apenergy.2014.10.087.

[79] R. Han, S. Xing, X. Wu, C. Pang, S. Lu, Y. Su, Q. Liu, C. Song, J. Gao, Relevant influence of alkali carbonate doping on the thermochemical energy storage of Ca-based natural minerals during CaO/$CaCO_3$ cycles, Renew. Energy 181 (2022) 267–277, https://doi.org/10.1016/j.renene.2021.09.021.

[80] S.L. Hsieh, F.Y. Li, P.Y. Lin, D.E. Beck, R. Kirankumar, G.J. Wang, S. Hsieh, CaO recovered from eggshell waste as a potential adsorbent for greenhouse gas CO_2, J. Environ. Manag. 297 (2021) 113430, https://doi.org/10.1016/j.jenvman.2021.113430.

[81] D. Gong, Z. Zhang, T. Zhao, Decay on cyclic CO_2 capture performance of calcium-based sorbents derived from wasted precursors in multicycles, Energies 15 (2022) 1–15, https://doi.org/10.3390/en15093335.

[82] M. Mohamed, S. Yusup, M.A. Bustam, Synthesis of CaO-based sorbent from biomass for CO_2 capture in series of calcination-carbonation cycle, Procedia Eng. 148 (2016) 78–85, https://doi.org/10.1016/j.proeng.2016.06.438.

[83] W. Liu, J.S. Dennis, D.S. Sultan, S.A.T. Redfern, S.A. Scott, An investigation of the kinetics of CO_2 uptake by a synthetic calcium based sorbent, Chem. Eng. Sci. 69 (2012) 644–658, https://doi.org/10.1016/j.ces.2011.11.036.

[84] M.R. Mohammadi, H. Bahmaninia, S. Ansari, A. Hemmati-Sarapardeh, S. Norouzi-Apourvari, M. Schaffie, M. Ranjbar, Evaluation of asphaltene adsorption on minerals of dolomite and sandstone formations in two and three-phase systems, Adv. Geo-Energy Res. 5 (2021) 39–52, https://doi.org/10.46690/ager.2021.01.05.

[85] S. Srinivasan, D. Dodson, M.B.J. Charles, S.L. Wallen, G. Albarelli, A. Kaushik, N. Hickman, G.R. Chaudhary, E. Stefanakos, J. Dhau, Energy storage in earth-abundant dolomite minerals, Appl. Sci. 10 (2020) 6679, https://doi.org/10.3390/APP10196679.

[86] A.A. Ayodeji, M.E. Ojewumi, B. Rasheed, J.M. Ayodele, Data on CaO and eggshell catalysts used for biodiesel production, Data Brief 19 (2018) 1466–1473, https://doi.org/10.1016/j.dib.2018.06.028.

[87] N. Tangboriboon, W. Unjan, W. Sangwan, A. Sirivat, Preparation of anhydrite from eggshell via pyrolysis, Green Process. Synth. 7 (2018) 139–146, https://doi.org/10.1515/gps-2016-0159.

[88] N. Erdogan, H.A. Eken, Precipitated Calcium carbonate production, synthesis and properties, Physicochem. Probl. Miner. Process. 53 (2017) 57–68, https://doi.org/10.5277/ppmp170105.

[89] H. Jiang, H. Guo, P. Li, Y. Li, B. Yan, Preparation of CaMgAl-LDHs and mesoporous silica sorbents derived from blast furnace slag for CO_2 capture, RSC Adv. 9 (2019) 6054–6063, https://doi.org/10.1039/c8ra08458k.

[90] J. Cheng, J. Zhou, J. Liu, X. Cao, K. Cen, Physicochemical characterizations and desulfurization properties in coal combustion of three calcium and sodium industrial wastes, Energy Fuel. 23 (2009) 2506–2516, https://doi.org/10.1021/ef8007568.

[91] H.H.T. Vu, M.D. Khan, R. Chilakala, T.Q. Lai, T. Thenepalli, J.W. Ahn, D.U. Park, J. Kim, Utilization of lime mud waste from paper mills for efficient phosphorus removal, Sustain. Times 11 (2019) 1524, https://doi.org/10.3390/su11061524.

[92] R. Sun, Y. Li, C. Liu, X. Xie, C. Lu, Utilization of lime mud from paper mill as CO_2 sorbent in calcium looping process, Chem. Eng. J. 221 (2013) 124–132, https://doi.org/10.1016/j.cej.2013.01.068.

[93] R. Sun, R. Xiao, J. Ye, Kinetic analysis about the CO_2 capture capacity of lime mud from paper mill in calcium looping process, Energy Sci. Eng. 8 (2020) 4014–4024, https://doi.org/10.1002/ese3.792.

[94] X. Gong, T. Zhang, J. Zhang, Z. Wang, J. Liu, J. Cao, C. Wang, Recycling and utilization of calcium carbide slag - current status and new opportunities, Renew. Sustain. Energy Rev. 159 (2022) 112133, https://doi.org/10.1016/j.rser.2022.112133.

[95] J. Yu, L. Sun, C. Ma, Y. Qiao, H. Yao, Thermal degradation of PVC: a review, Waste Manag. 48 (2016) 300–314, https://doi.org/10.1016/j.wasman.2015.11.041.

[96] Y. Wang, B. Ye, Z. Hong, Y. Wang, M. Liu, Uniform calcite mircro/nanorods preparation from carbide slag using recyclable citrate extractant, J. Clean. Prod. 253 (2020) 119930, https://doi.org/10.1016/j.jclepro.2019.119930.

[97] Z. Sun, R. Feng, L. Zhang, H. Xie, CO_2 capture and sequestration by sodium humate and $Ca(OH)_2$ from carbide slag, Res. Chem. Intermed. 44 (2018) 3613–3627, https://doi.org/10.1007/s11164-018-3328-x.

[98] H. Gupta, D.N. Yadav, I.M. Chaurasia, D.K. Singh, A. Maurya, A. Nishad, R. Dubey, "Use of blast furnace slag in concrete – a review ,", Int. J. Adv. Res. Sci. Eng. 7 (2018) 295–303.

[99] J. Dzięcioł, M. Radziemska, Blast furnace slag, post-industrial waste or valuable building materials with remediation potential? Minerals 12 (2022) 478, https://doi.org/10.3390/min12040478.

[100] S. Yasipourtehrani, S. Tian, V. Strezov, T. Kan, T. Evans, Development of robust CaO-based sorbents from blast furnace slag for calcium looping CO_2 capture, Chem. Eng. J. 387 (2020) 124140, https://doi.org/10.1016/j.cej.2020.124140.

[101] S.M. Abdelbasir, M.A.A. Khalek, From waste to waste: iron blast furnace slag for heavy metal ions removal from aqueous system, Environ. Sci. Pollut. Res. 29 (2022) 57964–57979, https://doi.org/10.1007/s11356-022-19834-3.

[102] C.I.C. Pinheiro, A. Fernandes, C. Freitas, E.T. Santos, M.F. Ribeiro, Waste marble powders as promising inexpensive natural CaO-based sorbents for post-combustion CO_2 capture, Ind. Eng. Chem. Res. 55 (2016) 7860–7872, https://doi.org/10.1021/acs.iecr.5b04574.

[103] P. Teixeira, C.I.C. Pinheiro, A. Fernandes, F. Ribeiro, Sustainable use of natural geological materials and marble wastes as promising calcium looping sorbents for CO_2 capture in the cement industry: comparative study, in: 14th Greenh. Gas Control Technol, Conf. Melb. 21-26, 2018, https://doi.org/10.2139/ssrn.3332630. Oct. 2018.

[104] Y. Li, H. Liu, R. Sun, S. Wu, C. Lu, Thermal analysis of cyclic carbonation behavior of CaO derived from carbide slag at high temperature, J. Therm. Anal. Calorim. 110 (2012) 685–694, https://doi.org/10.1007/s10973-011-1901-2.

[105] A. Nawar, H. Ghaedi, M. Ali, M. Zhao, N. Iqbal, R. Khan, Recycling waste-derived marble powder for CO_2 capture, Process Saf. Environ. Protect. 132 (2019) 214–225, https://doi.org/10.1016/j.psep.2019.10.005.

[106] F.N. Ridha, V. Manovic, Y. Wu, A. Macchi, E.J. Anthony, International journal of greenhouse gas control post-combustion CO_2 capture by formic acid-modified CaO-based sorbents, Int. J. Greenh. Gas Control 16 (2013) 21–28, https://doi.org/10.1016/j.ijggc.2013.02.026.

[107] F.N. Ridha, V. Manovic, A. Macchi, M.A. Anthony, E.J. Anthony, Assessment of limestone treatment with organic acids for CO_2 capture in Ca-looping cycles, Fuel Process, Technol. 116 (2013) 284–291, https://doi.org/10.1016/j.fuproc.2013.07.007.

[108] C. Sun, X. Yan, Y. Li, J. Zhao, Z. Wang, T. Wang, Coupled CO_2 capture and thermochemical heat storage of CaO derived from calcium acetate, Greenh. Gases Sci. Technol. 10 (2020) 1027–1038, https://doi.org/10.1002/ghg.2021.

[109] Y. Hu, W. Liu, J. Sun, M. Li, X. Yang, Y. Zhang, X. Liu, M. Xu, Structurally improved CaO-based sorbent by organic acids for high temperature CO_2 capture, Fuel 167 (2016) 17–24, https://doi.org/10.1016/j.fuel.2015.11.048.

[110] J. Miranda-Pizarro, A. Perejón, J.M. Valverde, L.A. Pérez-Maqueda, P.E. Sánchez-Jiménez, CO_2 capture performance of Ca-Mg acetates at realistic Calcium Looping conditions, Fuel 196 (2017) 497–507, https://doi.org/10.1016/j.fuel.2017.01.119.

[111] R. Sun, Y. Li, S. Wu, C. Liu, H. Liu, C. Lu, Enhancement of CO_2 capture capacity by modifying limestone with propionic acid, Powder Technol. 233 (2013) 8–14, https://doi.org/10.1016/j.powtec.2012.08.011.

[112] Y. Li, R. Sun, H. Liu, C. Lu, Cyclic CO_2 capture behavior of limestone modified with pyroligneous acid (PA) during calcium looping cycles, Ind. Eng. Chem. Res. 50 (2011) 10222–10228, https://doi.org/10.1021/ie2007455.

[113] K. Wang, F. Gu, P.T. Clough, P. Zhao, E.J. Anthony, CO_2 capture performance of gluconic acid modified limestone-dolomite mixtures under realistic conditions, Energy Fuel. 33 (2019) 7550–7560, https://doi.org/10.1021/acs.energyfuels.9b01256.

[114] T. Papalas, A.N. Antzaras, A.A. Lemonidou, Evaluation of calcium-based sorbents derived from natural ores and industrial wastes for high-temperature CO_2 capture, Ind. Eng. Chem. Res. 59 (2020) 9926–9938, https://doi.org/10.1021/acs.iecr.9b06834.

[115] B. González, J. Blamey, M. McBride-Wright, N. Carter, D. Dugwell, P. Fennell, J.C. Abanades, Calcium looping for CO_2 capture: sorbent enhancement through doping, Energy Proc. 4 (2011) 402–409, https://doi.org/10.1016/j.egypro.2011.01.068.

[116] Y. Xu, F. Donat, C. Luo, J. Chen, A. Kierzkowska, M. Awais Naeem, L. Zhang, C.R. Müller, Investigation of K_2CO_3-modified CaO sorbents for CO_2 capture using in-situ X-ray diffraction, Chem. Eng. J. 453 (2023) 139913, https://doi.org/10.1016/j.cej.2022.139913.

[117] E.P. Reddy, P.G. Smirniotis, High-temperature sorbents for CO_2 made of alkali metals doped on CaO supports, J. Phys. Chem. B 108 (2004) 7794–7800, https://doi.org/10.1021/jp031245b.

[118] Y. Xu, C. Luo, H. Sang, B. Lu, F. Wu, X. Li, L. Zhang, Structure and surface insight into a temperature-sensitive CaO-based CO_2 sorbent, Chem. Eng. J. 435 (2022) 134960, https://doi.org/10.1016/j.cej.2022.134960.

[119] L. Morona, M. Erans, D.P. Hanak, Effect of seawater, aluminate cement, and alumina-rich spinel on pelletized CaO-based sorbents for calcium looping, Ind. Eng. Chem. Res. 58 (2019) 11910–11919, https://doi.org/10.1021/acs.iecr.9b00944.

[120] B. González, J. Kokot-Blamey, P. Fennell, Enhancement of CaO-based sorbent for CO_2 capture through doping with seawater, Greenh. Gases Sci. Technol. 10 (2020) 878–883, https://doi.org/10.1002/ghg.2013.

[121] Y. Xu, C. Luo, Y. Zheng, H. Ding, D. Zhou, L. Zhang, Natural calcium-based sorbents doped with sea salt for cyclic CO_2 capture, Chem. Eng. Technol. 40 (2017) 522–528, https://doi.org/10.1002/ceat.201500330.

[122] C. Chi, Y. Li, W. Zhang, Z. Wang, Synthesis of a hollow microtubular Ca/Al sorbent with high CO_2 uptake by hard templating, Appl, Energy 251 (2019) 113382, https://doi.org/10.1016/j.apenergy.2019.113382.

[123] S. Wei, R. Han, Y. Su, J. Gao, G. Zhao, Y. Qin, Size effect of calcium precursor and binder on CO_2 capture of composite CaO-based pellets, Energy Proc. 158 (2019) 5073–5078, https://doi.org/10.1016/j.egypro.2019.01.641.

[124] P. Teixeira, C. Bacariza, I. Mohamed, C.I.C. Pinheiro, Improved performance of modified CaO-Al_2O_3 based pellets for CO_2 capture under realistic Ca-looping conditions, J. CO_2 Util. 61 (2022) 102007, https://doi.org/10.1016/j.jcou.2022.102007.

[125] A.A. Khosa, J. Yan, C.Y. Zhao, Investigating the effects of ZnO dopant on the thermodynamic and kinetic properties of $CaCO_3$/CaO TCES system, Energy 215 (2021) 119132, https://doi.org/10.1016/j.energy.2020.119132.

[126] B. Sarrión, A. Perejón, P.E. Sánchez-Jiménez, L.A. Pérez-Maqueda, J.M. Valverde, Role of calcium looping conditions on the performance of natural and synthetic Ca-based materials for energy storage, J. CO_2 Util. 28 (2018) 374–384, https://doi.org/10.1016/j.jcou.2018.10.018.

[127] Z. Bian, Y. Li, C. Sun, C. Zhang, Z. Wang, W. Liu, CaO/H_2O thermochemical heat storage capacity of a CaO/CeO_2 composite from CO_2 capture cycles, Ind. Eng. Chem. Res. 59 (2020) 16741–16750, https://doi.org/10.1021/acs.iecr.0c02340.

[128] A. Coppola, A. Esposito, F. Montagnaro, M. Iuliano, F. Scala, P. Salatino, The combined effect of H_2O and SO_2 on CO_2 uptake and sorbent attrition during fluidised bed calcium looping, Proc. Combust. Inst. 37 (2019) 4379–4387, https://doi.org/10.1016/j.proci.2018.08.013.

[129] A. Coppola, E. Gais, G. Mancino, F. Montagnaro, F. Scala, P. Salatino, Effect of steam on the performance of Ca-based sorbents in calcium looping processes, Powder Technol. 316 (2017) 578–584, https://doi.org/10.1016/j.powtec.2016.11.062.

[130] A. Coppola, M. Allocca, F. Montagnaro, F. Scala, P. Salatino, The effect of steam on CO_2 uptake and sorbent attrition in fluidised bed calcium looping: the influence of process conditions and sorbent properties, Sep. Purif. Technol. 189 (2017) 101–107, https://doi.org/10.1016/j.seppur.2017.08.001.

[131] Y. Li, X. Ma, W. Wang, C. Chi, J. Shi, L. Duan, Enhanced CO_2 capture capacity of limestone by discontinuous addition of hydrogen chloride in carbonation at calcium looping conditions, Chem. Eng. J. 316 (2017) 438–448, https://doi.org/10.1016/j.cej.2017.01.127.

[132] R.T. Symonds, D.Y. Lu, A. Macchi, R.W. Hughes, E.J. Anthony, The effect of HCl and steam on cyclic CO_2 capture performance in calcium looping systems, Chem. Eng. Sci. 242 (2021) 113762, https://doi.org/10.1016/j.ces.2017.08.019.

[133] A. Recio, S. Liew, D. Lu, R. Rahman, A. Macchi, J. Hill, The effects of thermal treatment and steam addition on integrated CuO/CaO chemical looping combustion for CO_2 capture, Technologies 4 (2016) 11, https://doi.org/10.3390/technologies4020011.

[134] M. Li, C. Shen, J. Ji, L. Li, Y. Wu, Multiple activation mechanisms of CaO-based sorbents promoted by pre-sintering-hydration, J. Environ. Chem. Eng. 10 (2022) 108216, https://doi.org/10.1016/j.jece.2022.108216.

[135] Y. Li, X. Xie, C. Liu, S. Niu, Cyclic carbonation properties of CMA as CO_2 sorbent at high temperatures, Adv. Mater. Res. 518–523 (2012) 655–658, https://doi.org/10.4028/www.scientific.net/AMR.518-523.655.

[136] K. Wang, X. Hu, P. Zhao, Z. Yin, Natural dolomite modified with carbon coating for cyclic high-temperature CO_2 capture, Appl. Energy 165 (2016) 14–21, https://doi.org/10.1016/j.apenergy.2015.12.071.

[137] S. Bai, J. Sun, L. Liu, Y. Da, Z. Zhou, R. Wang, Y. Guo, C. Zhao, Dolomite-derived composites doped with binary ions for direct solar thermal conversion and stabilized thermochemical energy storage, Sol. Energy Mater. Sol. Cells 239 (2022) 111659, https://doi.org/10.1016/j.solmat.2022.111659.

[138] C. Shen, C. Luo, T. Luo, J. Xu, B. Lu, S. Liu, L. Zhang, Effect of sodium bromide on CaO-based sorbents derived from three kinds of sources for CO_2 capture, ACS Omega 5 (2020) 17908–17917, https://doi.org/10.1021/acsomega.0c00219.

[139] Y. Xu, C. Shen, B. Lu, C. Luo, F. Wu, X. Li, L. Zhang, Study on the effect of NaBr modification on CaO-based sorbent for CO_2 capture and SO_2 capture, Carbon Capture, Sci. Technol. 1 (2021) 100015, https://doi.org/10.1016/j.ccst.2021.100015.

[140] J. Sun, Y. Yang, Y. Guo, Y. Xu, W. Li, C. Zhao, W. Liu, P. Lu, Stabilized CO_2 capture performance of wet mechanically activated dolomite, Fuel 222 (2018) 334–342, https://doi.org/10.1016/j.fuel.2018.02.162.

[141] M. Iyer, L. Fan, High Temperature CO_2 Capture Using Engineered Eggshells:a Route to Carbon Management, vol. 2, United States Patent, US, 2010.

[142] M. Imani, M. Tahmasebpoor, P.E. Sánchez-Jiménez, J.M. Valverde, V. Moreno, Improvement in cyclic CO_2 capture performance and fluidization behavior of eggshell-derived $CaCO_3$ particles modified with acetic acid used in calcium looping process, J. CO_2 Util. 65 (2022) 102207, https://doi.org/10.1016/j.jcou.2022.102207.

[143] A. Nawar, M. Ali, A.H. Khoja, A. Waqas, M. Anwar, M. Mahmood, Enhanced CO_2 capture using organic acid structure modified waste eggshell derived CaO sorbent, J. Environ. Chem. Eng. 9 (2021) 104871, https://doi.org/10.1016/j.jece.2020.104871.

[144] Y. Xu, T. Zhang, B. Lu, C. Luo, F. Wu, X. Li, L. Zhang, Glycine tailored effective CaO-based heat carriers for thermochemical energy storage in concentrated solar power plants, Energy Convers. Manag. 250 (2021) 114886, https://doi.org/10.1016/j.enconman.2021.114886.

[145] A. Nawar, M. Ali, M. Mahmood, M. Anwar, Z.A. Khan, Effect of structural promoters on calcium based sorbents from waste derived sources, Mater. Today Commun. 24 (2020) 101075, https://doi.org/10.1016/j.mtcomm.2020.101075.

[146] C. Huang, M. Xu, X. Huai, Z. Liu, Hierarchically porous calcium-based composites synthesized by eggshell membrane templating for thermochemical energy storage of concentrated solar power, J. Energy Storage 52 (2022) 104769, https://doi.org/10.1016/j.est.2022.104769.

[147] M. Imani, M. Tahmasebpoor, P. Enrique Sánchez-Jiménez, J. Manuel Valverde, V. Moreno, A novel, green, cost-effective and fluidizable SiO2-decorated calcium-based adsorbent recovered from eggshell waste for the CO_2 capture process, Sep. Purif. Technol. 305 (2023) 122523, https://doi.org/10.1016/j.seppur.2022.122523.

[148] S.Y. Shan, A.H. Ma, Y.C. Hu, Q.M. Jia, Y.M. Wang, J.H. Peng, Development of sintering-resistant CaO-based sorbent derived from eggshells and bauxite tailings for cyclic CO_2 capture, Environ. Pollut. 208 (2016) 546–552, https://doi.org/10.1016/j.envpol.2015.10.028.

[149] C. Qin, W. Liu, H. An, J. Yin, B. Feng, Fabrication of CaO-based sorbents for CO_2 capture by a mixing method, Environ. Sci. Technol. 46 (2012) 1932–1939, https://doi.org/10.1021/es203525y.

[150] M. Mohammadi, P. Lahijani, A.R. Mohamed, Refractory dopant-incorporated CaO from waste eggshell as sustainable sorbent for CO_2 capture: experimental and kinetic studies, Chem. Eng. J. 243 (2014) 455–464, https://doi.org/10.1016/j.cej.2014.01.018.

[151] H. Lu, A. Khan, S.E. Pratsinis, P.G. Smirniotis, C. Zu, Flame-Made Durable Doped-CaO Nanosorbents for CO2 Capture, 96, 2009, pp. 1093–1100.

[152] P. Jamrunroj, S. Wongsakulphasatch, A. Maneedaeng, C.K. Cheng, S. Assabumrungrat, Surfactant assisted CaO-based sorbent synthesis and their application to high-temperature CO_2 capture, Powder Technol. 344 (2019) 208–221, https://doi.org/10.1016/j.powtec.2018.12.011.

[153] N. Tangboriboon, R. Kunanuruksapong, A. Sirivat, R. Kunanuruksapong, A. Sirivat, Preparation and properties of calcium oxide from eggshells via calcination, Mater. Sci. Pol. 30 (2012) 313–322, https://doi.org/10.2478/s13536-012-0055-7.

[154] Y.F. Huang, Y.T. Lee, P. Te Chiueh, S.L. Lo, Microwave calcination of waste oyster shells for CO_2 capture, Energy Proc. 152 (2018) 1242–1247, https://doi.org/10.1016/j.egypro.2018.09.176.

[155] J. Arcenegui-Troya, P.E. Sánchez-Jiménez, A. Perejón, J.M. Valverde, R. Chacartegui, L.A. Pérez-Maqueda, Calcium-looping performance of biomineralized $CaCO_3$ for CO_2 capture and thermochemical energy storage, Ind. Eng. Chem. Res. 59 (2020) 12924–12933, https://doi.org/10.1021/acs.iecr.9b05997.

[156] O. Awogbemi, F. Inambao, E.I. Onuh, Modification and characterization of chicken eggshell for possible catalytic applications, Heliyon 6 (2020) e05283, https://doi.org/10.1016/j.heliyon.2020.e05283.

[157] V. Manovic, E.J. Anthony, G. Grasa, J.C. Abanades, CO_2 looping cycle performance of a high-purity limestone after thermal activation/doping, Energy Fuel. 22 (2008) 3258–3264, https://doi.org/10.1021/ef800316h.

[158] R. Sun, Y. Li, J. Zhao, C. Liu, C. Lu, CO_2 capture using carbide slag modified by propionic acid in calcium looping process for hydrogen production, Int. J. Hydrogen Energy 38 (2013) 13655–13663, https://doi.org/10.1016/j.ijhydene.2013.08.030.

[159] S. R, S.W.S. Changtian Liu, Yingjie Li, Cyclic CO_2 capture of carbide slag modified by pyroligneous acid in calcium looping cycles, Asia-Pacific, J. Chem. Eng. 9 (2014) 678–685, https://doi.org/10.1002/apj.

[160] J.M. Valverde, J. Miranda-Pizarro, A. Perejón, P.E. Sánchez-Jiménez, L.A. Pérez-Maqueda, Calcium-Looping performance of steel and blast furnace slags for thermochemical energy storage in concentrated solar power plants, J. CO_2 Util. 22 (2017) 143–154, https://doi.org/10.1016/j.jcou.2017.09.021.

[161] J. Miranda-Pizarro, A. Perejón, J.M. Valverde, P.E. Sánchez-Jiménez, L.A. Pérez-Maqueda, Use of steel slag for CO_2 capture under realistic calcium-looping conditions, RSC Adv. 6 (2016) 37656–37663, https://doi.org/10.1039/c6ra03210a.

[162] Y. Zhang, L. He, A. Ma, Q. Jia, S. He, S. Shan, CaO-based sorbent derived from lime mud and bauxite tailings for cyclic CO_2 capture, Environ. Sci. Pollut. Res. 25 (2018) 28015–28024, https://doi.org/10.1007/s11356-018-2825-1.

[163] X. Ma, Y. Li, C. Zhang, Z. Wang, Development of Mn/Mg-copromoted carbide slag for efficient CO_2 capture under realistic calcium looping conditions, Process Saf. Environ. Protect. 141 (2020) 380–389, https://doi.org/10.1016/j.psep.2020.05.051.

[164] W. Zhang, X. Ma, Y. Li, J. Zhao, Z. Wang, A study of the synergistic effects of Mn/steam on CO_2 capture performance of CaO by experiment and DFT calculation, Greenh. Gases Sci. Technol. 9 (2019) 409–423, https://doi.org/10.1002/ghg.1859.

[165] Y. Wang, Y. Li, L. Yang, X. Fan, L. Chu, $Ca_{12}Al_{14}O_{33}$ or MgO supported Ni-carbide slag bi-functional materials for H_2 production and CO_2 capture in sorption-enhanced steam gasification of cellulose/polyethylene mixture, Fuel 328 (2022) 125209, https://doi.org/10.1016/j.fuel.2022.125209.

[166] X. Ma, Y. Li, Y. Qian, Z. Wang, Sorbent prepared by the hydrothermal template, Energies 12 (2019) 2617.

[167] Z. He, Y. Li, W. Zhang, X. Ma, L. Duan, H. Song, Effect of re-carbonation on CO_2 capture by carbide slag and energy consumption in the calciner, Energy Convers. Manag. 148 (2017) 1468–1477, https://doi.org/10.1016/j.enconman.2017.07.006.

[168] B. Arias, G. Grasa, J.C. Abanades, V. Manovic, E.J. Anthony, The effect of steam on the fast carbonation reaction rates of CaO, Ind. Eng. Chem. Res. 51 (2012) 2478–2482, https://doi.org/10.1021/ie202648p.

[169] W. Zhang, Y. Li, Z. He, X. Ma, H. Song, CO_2 capture by carbide slag calcined under high-concentration steam and energy requirement in calcium looping conditions, Appl. Energy 206 (2017) 869–878, https://doi.org/10.1016/j.apenergy.2017.08.236.

[170] S. Haran, A.B. Rao, R. Banerjee, Techno-economic analysis of a 660 MWe supercritical coal power plant in India retrofitted with calcium looping (CaL) based CO_2 capture system, Int. J. Greenh. Gas Control 112 (2021) 103522, https://doi.org/10.1016/j.ijggc.2021.103522.

[171] X. Guo, P. Zheng, X. Zou, X. Chen, Q. Zhang, Influence of pyroligneous acid on fermentation parameters, CO_2 production and bacterial communities of rice straw and stylo silage, Front. Microbiol. 12 (2021) 701434, https://doi.org/10.3389/fmicb.2021.701434.

[172] I.A. Palasantzas, D.L. Wise, Preliminary economic analysis for production of calcium magnesium acetate from organic residues, Resour. Conserv. Recycl. 11 (1994) 225–243, https://doi.org/10.1016/0921-3449(94)90092-2.

[173] S.T. Yang, H. Zhu, V.P. Lewis, I.C. Tang, Calcium magnesium acetate (CMA) production from whey permeate: process and economic analysis, Resour. Conserv. Recycl. 7 (1992) 181–200, https://doi.org/10.1016/0921-3449(92)90016-U.

[174] US20080206128A1 - US Patent Magnesium oxide.Pdf, (n.d.).

[175] S. Pourrahim, A. Salem, S. Salem, R. Tavangar, Application of solid waste of ductile cast iron industry for treatment of wastewater contaminated by reactive blue dye via appropriate nano-porous magnesium oxide, Environ. Pollut. 256 (2020) 113454, https://doi.org/10.1016/j.envpol.2019.113454.

[176] A. Gil, E. Arrieta, M.Á. Vicente, S.A. Korili, Application of industrial wastes from chemically treated aluminum saline slags as adsorbents, ACS Omega 3 (2018) 18275–18284, https://doi.org/10.1021/acsomega.8b02397.

[177] M. Satish Reddy, D. Neeraja, Aluminum residue waste for possible utilisation as a material: a review, Sadhana - Acad. Proc. Eng. Sci. 43 (2018) 1–8, https://doi.org/10.1007/s12046-018-0866-2.

[178] P.F. Gouveia, L.M. Schabbach, J.C.M. Souza, B. Henriques, J.A. Labrincha, F.S. Silva, M.C. Fredel, J. Mesquita-Guimarães, New perspectives for recycling dental zirconia waste resulting from CAD/CAM manufacturing process, J. Clean. Prod. 152 (2017) 454–463, https://doi.org/10.1016/j.jclepro.2017.03.117.

[179] S. Tian, J. Jiang, F. Yan, K. Li, X. Chen, Synthesis of highly efficient CaO-based, self-stabilizing CO_2 sorbents via structure-reforming of steel slag, Environ. Sci. Technol. 49 (2015) 7464–7472, https://doi.org/10.1021/acs.est.5b00244.

[180] X. Ma, Y. Li, C. Chi, W. Zhang, J. Shi, L. Duan, CO_2 capture performance of mesoporous synthetic sorbent fabricated using carbide slag under realistic calcium looping conditions, Energy Fuel. 31 (2017) 7299–7308, https://doi.org/10.1021/acs.energyfuels.7b00676.

[181] A. Kurlov, A. Armutlulu, F. Donat, A.R. Studart, C.R. Müller, CaO-based CO_2 sorbents with a hierarchical porous structure made via microfluidic droplet templating, Ind. Eng. Chem. Res. 59 (2020) 7182–7188, https://doi.org/10.1021/acs.iecr.9b05996.

[182] V.V. Rodaev, S.S. Razlivalova, Performance and durability of the zr-doped cao sorbent under cyclic carbonation–decarbonation at different operating parameters, Energies 14 (2021), https://doi.org/10.3390/en14164822.

[183] S.M. Hashemi, D. Karami, N. Mahinpey, Solution combustion synthesis of zirconia-stabilized calcium oxide sorbents for CO_2 capture, Fuel 269 (2020) 117432, https://doi.org/10.1016/j.fuel.2020.117432.

[184] S.M. Hashemi, R. Zhou, N. Mahinpey, Evaluation of MgO- and $CaZrO_3$-promoted CaO-based pellets produced via solution combustion synthesis, Chem. Eng. J. 450 (2022) 138274, https://doi.org/10.1016/j.cej.2022.138274.

[185] M.A. Naeem, A. Armutlulu, Q. Imtiaz, F. Donat, R. Schäublin, A. Kierzkowska, C.R. Müller, Optimization of the structural characteristics of CaO and its effective stabilization yield high-capacity CO_2 sorbents, Nat. Commun. 9 (2018) 1–11, https://doi.org/10.1038/s41467-018-04794-5.

[186] V. V Rodaev, S.S. Razlivalova, A.I. Tyurin, V.M. Vasyukov, Electrospun Zr-Doped CaO Sorbent for CO_2 Capture, 2023.

[187] C. Huang, M. Xu, X. Huai, Z. Liu, Template-free synthesis of hollow CaO/Ca_2SiO_4 nanoparticle as a cyclically stable high-capacity CO_2 sorbent, ACS Sustain. Chem. Eng. 9 (2021) 2171–2179, https://doi.org/10.1021/acssuschemeng.0c07689.

[188] S.B. Mousavi, M. Heidari, F. Rahmani, R. Akbari Sene, P.T. Clough, S. Ozmen, Highly robust Zr-stabilized CaO nanoadsorbent prepared via a facile one-pot MWCNT-based method for CO_2 capture under realistic calcium looping conditions, J. Clean. Prod. 384 (2023) 135579, https://doi.org/10.1016/j.jclepro.2022.135579.

[189] V. Jani, A. Rasyotra, H. Gunda, C. Ghoroi, K. Jasuja, Titanium diboride (TiB2) derived nanosheets enhance the CO_2 capturing ability of Calcium Oxide (CaO), Ceram. Int. 48 (2022) 32380–32388, https://doi.org/10.1016/j.ceramint.2022.07.181.

[190] J. Wang, P. Wu, Y. Wei, Q. Zhao, P. Ning, Y. Huang, S. Wen, J. Xu, Q. Wang, Study of calcium-based CO_2 sorbent with high cycling stability derived from steel slag and its anti-sintering mechanism, J. CO_2 Util. 66 (2022) 102279, https://doi.org/10.1016/j.jcou.2022.102279.

[191] R. Barker, The reversibility of the reaction, J. Appl. Chem. Biotechnol. 23 (1973) 133–142.

[192] N.H. Florin, A.T. Harris, Reactivity of CaO derived from nano-sized $CaCO_3$ particles through multiple CO_2 capture-and-release cycles, Chem. Eng. Sci. 64 (2009) 187–191, https://doi.org/10.1016/j.ces.2008.10.021.

[193] J.D. Durán-Martín, P.E. Sánchez Jimenez, J.M. Valverde, A. Perejón, J. Arcenegui-Troya, P. García Triñanes, L.A. Pérez Maqueda, Role of particle size on the multicycle calcium looping activity of limestone for thermochemical energy storage, J. Adv. Res. 22 (2020) 67–76, https://doi.org/10.1016/j.jare.2019.10.008.

[194] Y. Zhou, Y. Chen, W. Li, K. Li, Z. Jia, J. Sun, C. Zhao, High-temperature CO_2 uptake and mechanical strength enhancement of the calcium aluminate cement-bound carbide slag pellets, Energy Fuel. 35 (2021) 8117–8125, https://doi.org/10.1021/acs.energyfuels.1c00355.

[195] Y. Long, J. Sun, C. Mo, X. She, P. Zeng, H. Xia, J. Zhang, Z. Zhou, X. Nie, C. Zhao, One-step fabricated Zr-supported, CaO-based pellets via graphite-moulding method for regenerable CO_2 capture, Sci. Total Environ. 851 (2022) 158357, https://doi.org/10.1016/j.scitotenv.2022.158357.

[196] N. Wang, Y. Feng, L. Liu, X. Guo, Effects of preparation methods on the structure and property of Al-stabilized CaO-based sorbents for CO_2 capture, Fuel Process. Technol. 173 (2018) 276–284, https://doi.org/10.1016/j.fuproc.2018.02.005.

[197] Y. Wang, M.Z. Memon, Q. Xie, Y. Gao, A. Li, W. Fu, Z. Wu, Y. Dong, G. Ji, Study on CO_2 sorption performance and sorption kinetics of Ce- and Zr-doped CaO-based sorbents, Carbon Capture Sci. Technol. 2 (2022) 100033, https://doi.org/10.1016/j.ccst.2022.100033.

[198] Y. Long, J. Sun, C. Mo, X. She, P. Zeng, H. Xia, J. Zhang, Z. Zhou, X. Nie, C. Zhao, One-step fabricated Zr-supported, CaO-based pellets via graphite-moulding method for regenerable CO_2 capture, Sci. Total Environ. 851 (2022) 158357, https://doi.org/10.1016/j.scitotenv.2022.158357.

[199] R. Rajamathi, C. Nethravathi, Porous CaO–MgO nanostructures for CO_2 capture, ACS Appl. Nano Mater. 4 (2021) 10969, https://doi.org/10.1021/acsanm.1c02428.

[200] D. Baciu, T. Steriotis, G. Charalambopoulou, A. Stubos, The effect of hydrothermal treatment on the structure and CO_2 uptake capacity of CaO-based sorbents, J. Optoelectron. Adv. Mater. 18 (2016) 378–382.

[201] S. Wei, R. Han, Y. Su, J. Gao, G. Zhao, Y. Qin, Pore structure modified CaO-based sorbents with different sized templates for CO_2 capture, Energy Fuel. 33 (2019) 5398–5407, https://doi.org/10.1021/acs.energyfuels.9b00747.